1994

A Spectroscopic Study of OB+ Stars.

Jyotsna Vijapurkar
Louisiana State University and Agricultural & Mechanical College

Order Number 9502152

A spectroscopic study of OB^{+} stars

Vijapurkar, Jyotsna, Ph.D.

The Louisiana State University and Agricultural and Mechanical Col., 1994

U·M·I
300 N. Zeeb Rd.
Ann Arbor, MI 48106

A SPECTROSCOPIC STUDY OF OB$^+$ STARS

A Dissertation

Submitted to the Faculty of the
Louisiana State University and
Agricultural and Mechanical College
in partial fulfillment of the
requirements for the degree of
Doctor of Philosophy

in

The Department of Physics and Astronomy

by
Jyotsna Vijapurkar
B.Sc., Osmania University, Hyderabad, India 1980
M.S., Louisiana State University, 1989
May 1994

ACKNOWLEDGEMENTS

I am grateful to Prof. John Drilling for his help, guidance and patience over the years, without which this work would not have been possible.

I am thankful to Profs. Charles Perry, Arlo Landolt, Bill Metcalf and Juhan Frank, who offered many helpful suggestions and comments.

I am also thankful to all my fellow students who made my days here so much fun. Particular thanks to Horst Vath, Paul Fisher, Yingcai Peng, Dubravka Rupnik, Lijun Zhang and Evan Mauceli who were always ready to help when needed.

TABLE OF CONTENTS

ABSTRACT

We present here the results of an analysis of spectroscopic and photometric observations of OB^+ stars. These mostly luminous young stars were selected from a survey of the Milky Way that is complete to the 12th B magnitude and covers 360° of galactic longitude and ±10° of galactic latitude.

We determined the MK spectral types of 291 OB^+ stars; a detailed discussion of the MK system and the process of spectral classification is given. Using the MK types and UBV photometry, we derived the distances to these stars and to other OB^+ stars that had published MK spectral types. We thus have distances to nearly all of the non-emission OB^+ stars in the Milky Way down to the 12th B magnitude. We derive the space distribution of these stars and compare it with previous studies of Galactic structure. The color excesses derived from these data are plotted to show the distribution of dust in the Galactic plane out to several kpc.

As is often the case in surveys of this nature, several astrophysically interesting peculiar spectra were discovered, and these too are described.

CHAPTER 1

INTRODUCTION

O and B type stars are well known as useful tracers of spiral arms; they are luminous, massive stars that are short-lived and hence are found in the spiral arms where they were born. Because of their high luminosities, they can be seen to great distances, a particular advantage in the dusty Galactic disk where the absorption of light in the optical region is very high. They can also be picked out easily on very low resolution survey plates.

This project was initiated to study Galactic structure using OB^+ stars selected from the most complete survey to date, consisting of the survey by Stephenson and Sanduleak [1] which is complete to 12th photographic magnitude and covers the entire southern sky between galactic latitudes $\pm$ 10°, and the Case–Hamburg Luminous Star survey [2, 3, 4, 5, 6, 7] which covers the northern Milky Way. The OB^+ stars are those that showed very weak Balmer lines or no lines at all in their spectra on the objective prism survey plates. So they include (a) all those stars that do not have enough neutral hydrogen to produce strong Balmer lines: all O type and B0 stars of all luminosity classes, including very hot O-type subdwarfs, i.e. stars in which most of the hydrogen is ionized, and hydrogen-deficient stars, (b) some later B type supergiants because there is very little pressure broadening, (c) some later B type dwarfs with broad lines and (d) stars that have emission that partially or completely fills in the absorption lines. Approximately 10% of the stars in the catalogs referred to above are OB^+.

We determined MK spectral types of 291 of the southern OB^+ stars which did not have published spectral types at the time of observation. Then, using published UBV photometry, we determined the distances to these stars and to the stars that had published spectral types. Thus, in the southern Milky Way, we have distances to virtually all the OB^+ stars complete to the 12th photographic magnitude.

The distances were obtained using spectroscopic and photometric data. MK spectral types were determined from 62.5Å/mm classification spectrograms. The instrumental set-up with which the spectrograms were obtained is described in Chapter 2. A description of the classification process is given in Chapter 3. Once the spectral type of a star is known, its absolute magnitude M_V, and intrinsic color, $(B - V)_0$, can be determined from published calibrations. The apparent magnitude V and color B-V are known from the photometry. The distance d is then determined using the inverse square law:

$$V - M_V = 5\log d - 5 + A_V \tag{1.1}$$

where A_V is the interstellar extinction given by $A_V = R \cdot E_{B-V}$. E_{B-V} is the color excess, i.e. the difference between the observed and intrinsic colors, and R is a constant equal to 3.2 [8].

The distribution of the stars can then be plotted in the Galactic plane. These plots are shown in chapter 4. Also, since the amount of extinction along the line of sight to each star can be determined from this data, the distribution of dust can be plotted. This, too, is shown in Chapter 4.

There have been studies of the spiral structure of the Galaxy using other spiral arm tracers, some of which will be mentioned here. Spiral structure has been derived using 21-cm observations of H I, as done by Verschuur [9], but such maps depend on the adopted rotation curve of the Galaxy. Burton [10] has discussed in detail the problems involved in deriving the spiral structure from 21-cm observations. Georgelin and Georgelin [11] have published a map of the spiral arms using radio and optical data on HII regions. Walborn [12] has plotted the distribution of O stars in the solar neighborhood. Reed [13] has plotted the distribution of all OB stars using published UVBβ photometry.

The first attempt to map the spiral arms of the Galaxy was made several years ago by Morgan et al [14]; they used HII regions as tracers and published a brief description of the arms out to about 3 kpc. Optical studies in subsequent years have been limited to approximately this distance range, with the exception of Georgelin and Georgelin [11] whose optical data extends to 9 kpc in some directions. More recently, there has been further work both at optical and radio wavelengths; in particular, Reed [15] found an OB association at 6 kpc in the Puppis window at $l = 245°$ using UBV photometry of stars down to the 21st magnitude. Kimeswenger and Weinberger [16] found evidence for a spiral arm outside the Perseus arm using published data on spiral tracers. Most studies of Galactic structure and of the distribution of interstellar material have been restricted to specific longitude intervals. Comprehensive surveys, using homogeneous data, like the one reported here, are rare, and do not extend to as great a distance.

While this project started out as a study of Galactic structure using OB^+ stars as tracers, the most interesting outcome astrophysically has been identifying peculiar stars during spectral classification. These are discussed in Chapter 3. Among them are He stars, subdwarfs, and some variable stars, some of which have already been studied in detail.

CHAPTER 2

OBSERVATIONS

2.1 Spectroscopy

The Program Stars

Classification spectrograms of a total of 323 stars including standards of types O3 to A, of all luminosity classes, were obtained with the 1-meter image tube spectrograph at Cerro Tololo Inter-American Observatory(CTIO). The program stars were selected from the Case-Hamburg OB survey [3, 5, 7] and its extension to the southern Milky Way [1]. The survey is complete to 12th magnitude and covers the entire sky between Galactic latitudes $\pm 10°$. Most of the stars selected are from the Southern Milky Way catalog. Classification spectrograms were obtained of nearly all stars not showing Balmer emission that were brighter than B=12.0 (though a few that are fainter are also included), were classified as OB^+, were observable from CTIO, and for which MK spectral types were not available in the literature at the time of observation. Some stars with Balmer emission were also observed.

The 1-Meter Image Tube Spectrograph

A schematic diagram of the spectrograph, taken from the CTIO facilities manual, is shown in Fig. 1. Light from the telescope passes through one of a set of neutral density filters, then a skylight suppressor/rocker assembly, and comes to a focus on the slit. The neutral density filters available on the pre-slit filter wheel are 50 sq. mm filters of 1.25, 2.5, 5.0 and 7.5 magnitudes.

The skylight suppressor is a 0.51 mm wide slot that allows the stellar beam to pass through the slit jaws while blocking sky light. The rocker assembly is used for automatic widening of stellar spectra; it consists of a 25.4 mm quartz tilt plate that moves the image along the slit as the tilt angle is varied. The amount of widening can be chosen to be 0.17, 0.34, 0.67, 1.01 and 1.33 mm (at the plate).

The slit is 19 mm long and can be varied in width from 5 to 1200 microns. The slit length decker is used to choose the desired length of the slit; the comparison spectrum, which can be recorded simultaneously with the stellar spectrum, lies 0.33 mm on either side of the slit, and is 0.42 mm wide. (This was not used for the classification spectrograms so that they could be viewed next to the standard spectrum). A helium-argon glow lamp, a neon bulb and an iron-argon hollow cathode are available as comparison sources.

The beam from the slit falls on the collimator (after passing through a series of devices for slit viewing etc.) which sends a 90 mm parallel beam to the grating. The collimator is an off axis paraboloid of focal length 90 cm. It can be moved 0.91 cm for focusing. The gratings are Bausch and Lomb plane reflection gratings with 128×102 mm ruled area. Six different gratings are available with different values of ruling spacings and blaze. The dispersions range from 45 to 226Å/mm. The grating can be tilted (with respect to the incident beam) to change the wavelength falling at the center of the detector; tables of the tilt angle versus the central wavelength are given in the CTIO facilities manual.

The dispersed beam then passes through Newall masks (used for fine focusing and protecting the detector) and reaches the image-tube camera unit.

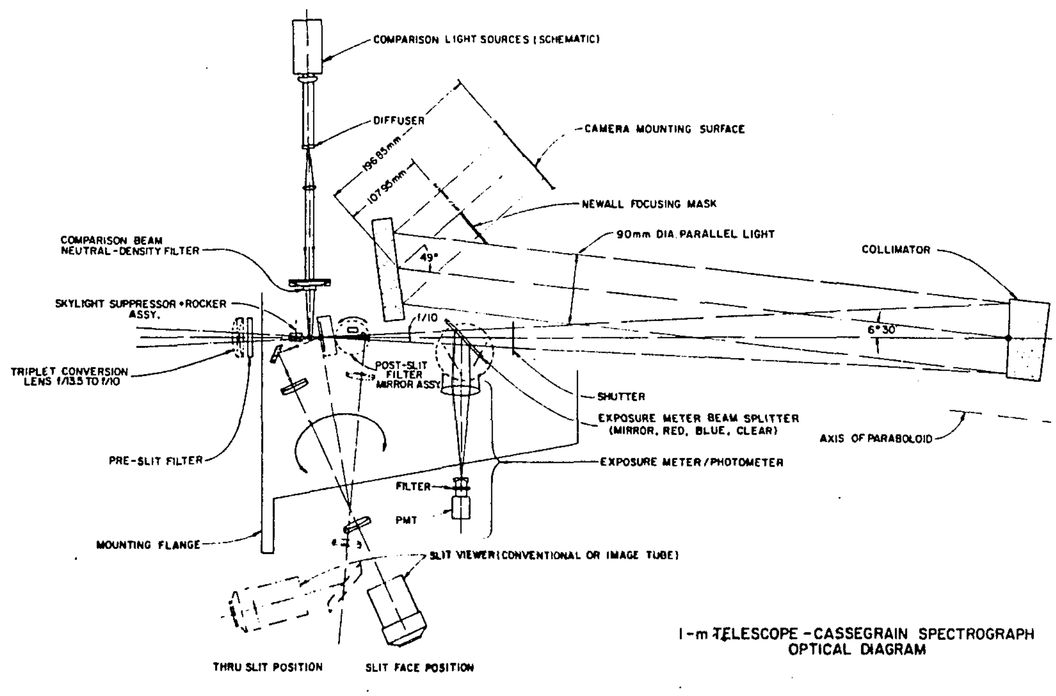

Figure 1: A schematic diagram of the 1m Image Tube Spectrograph.

The image tube is an RCA 33063 two stage intensifier with an S-20 photocathode and a fine grain P11 blue output screen. The intensified image on the phosphor screen of the image tube is brought to a focus on the photographic plate by a transfer lens. This Nikon lens, whose aperture stop can be varied from *f/1* to *f/16*, reimages the screen with unit magnification on the photographic plate.

Between the slit and the collimator are:

i) Post slit filter/mirror assembly. The mirror is used to direct the beam of light to the slit viewer. The viewer can be swiveled to two positions to view the slit either with light reflected off the slit jaws or the light entering the slit and deflected by the mirror. When this mirror is in position, no light reaches the collimator. There is also a choice of two slit viewers—conventional or image tube; the latter uses an RCA 4550 tube. A GG495 filter that blocks wavelengths below 5000Å is installed in this assembly, but can be replaced by any filter of appropriate dimensions.

ii) A beam splitter that can be positioned so that it sends to a photometer either (a) no light, (b) all the light from the beam, (c) $\approx$3.5 percent of the light from the beam while transmitting in the blue (3300 to 5000Å) region or (d) $\approx$ 4 percent of the beam while transmitting in the visual-red (5000 to 7000Å) region. The photomultiplier, with its display meter, serves as an exposure meter.

iii) A shutter.

For these observations, grating # 35 was used in second order; it has 600 lines/mm and blaze wavelength of 7500Å. The filter BG38 was used to suppress the first order spectrum. The spectra were recorded on IIIa-J photographic plates baked in nitrogen. The dispersion of the spectrograms is 62.5 Å/mm with a resolution of 2Å. The spectra were well widened, to about 1.0 mm to increase the signal to noise. Spectra of some standards were widened to more than 1.0 mm. Several spectra at different exposures were taken of each of the standards, so that while comparing the spectrum of a star with that of a standard, spectra of similar exposures could be compared. This is necessary because of the non-linear response of the photographic plate. Typically for the standards, which are bright, neutral density filters of 2.5 or 5 magnitudes were used.

In general, between 4 to 8 spectrograms were recorded on each plate. One spectrum of the iron-argon hollow cathode was recorded at the top of each plate, and this helped to define an order so that spectrum #1, 2 etc. could be identified as that of a particular star.

The observations reported here were made in 1978-79 by J. S. Drilling. It was considered best not to get new observations for the dissertation in view of the limited observing time available on the national telescopes, and the uncertainty of getting clear skies during the allotted time, but to use existing observations. Recently, the photographic detector has been replaced by a CCD detector. Observations were later made by the author with this new instrumental set-up for related investigations. Ultraviolet spectra of hot extreme He stars were also obtained by the author with the International Ultraviolet Explorer.

2.2 Photometry

UBV photometric observations were made by J. S. Drilling and have been published. The LSS stars were observed with the 0.4m and Lowell 0.6m telescopes at CTIO [17]. UBV photometry of the LS stars was obtained with the 41-cm telescope at Kitt Peak National Observatory [18].

CHAPTER 3

SPECTRAL CLASSIFICATION

3.1 The MK System

The MK system of spectral classification is a two dimensional system (of temperature and luminosity classes) defined by a set of standard stars. A spectral type is assigned to any given star by comparing it to the standard, which is observed with the same instrument as the program stars. While certain line ratios are used as the primary criteria in determining the spectral type, it is the appearance of the entire line spectrum that is important in this comparison. In other words, a spectral type as defined by the standard is assigned to a star if all the lines and blends in its spectrum, and not just one or two lines or line ratios, appear like those in the standard to within the error of the classification. A star is considered to be peculiar if it is impossible to match its entire spectrum to any standard. This does not mean that a temperature class and a luminosity class cannot be assigned to the star, but that additional dimensions are required to describe the peculiarity. The two dimensional spectral type is the one that the spectrum would look like if the peculiarity were to be ignored. (In deciding this, the features that are ignored are the minimum number that need to be 'thrown out' in order to match the spectrum to a standard's). For example, a star that looks very much like an O9 Ia standard except for the nitrogen lines which are very strong while the carbon lines are weak, may be described as ON9 Ia following Walborn [19]. Or a B0 V broadlined star with emission in the Balmer lines would be described as B0 Vne where the 'n' denotes line broadening.

Since the primary criteria help to pin down the star's two dimensional spectral type, what is considered to be a peculiarity, then, depends, to some extent, on what are chosen to be the primary criteria. The three (or more) dimensional spectral type is less arbitrary than the previous statement might imply, because whatever the choice of the primary criteria, it must be emphasised that, but for the peculiarity, the star's two-dimensional spectral type should match that of the standard's. The chosen primary criteria may be useful in picking out certain types of anomalies; the use of He and Si line ratios for spectral classification, for example, is particularly suited to pick out stars that have anomalous C, N or O line strengths, but not stars that have anomalous He or Si strengths. The important point is that the classification assigned to the star is descriptive of the appearance of the spectrum. This, in fact, is one of the fundamental properties of the MK system—that the type assigned to a star describes its spectrum without reference to theoretical interpretation.

The historical development of the MK system illustrates its empirical nature. The system of spectral classification was developed [20] before the Saha equation (published in 1920) was known. The stars were grouped together based on the similarity of their spectra, and the sequence of spectral types from O to M was based entirely on the smoothly varying appearance of the spectrum from one class to the next, and only later was this recognised to be a temperature sequence. Although it was suspected that some of the spectral features depended on luminosity, it was not until 1943 [21] that a second dimension of luminosity classes was added to the classification. Typical star(s) were cited for each class, which later gave rise to the standard stars which would define the system. The physical properties of the stars in each class may be determined by calibrations, but possible changes in these values through improved observations or theory do not affect the system.

In the old MK types [22] the earliest temperature class is O5 and no luminosity classification is given for the O5-O8 stars. A revised MK system, [23] defined by the 'dagger types' specifies the reference frame for the early type stars and has standards as early as O4 along with, for one star, ζ Puppis, the designation 'f', which denotes that the N III $\lambda\lambda$4634-42 and/or He II λ4686 lines appear in emission. The 'f' designation was first introduced by Plaskett and Pearce in 1931 and seems to have been used widely, though no Of standards were specified until 1973. The revised MK atlas [24], which differs from the earlier one in having only one standard for each class to better define the class, does specify luminosity classes If and V for the O4 to O8 temperature classes.

Walborn, using a higher dispersion (63.5Å/mm) and resolution (1Å) has extended the temperature class to O3 [25] and shown a correspondence between the 'f' designation and luminosity [26]. However there is a discrepancy in at least one case between Walborn's type and the MK system; the star ζ Puppis is a MK standard of type O5 If but has been classified as O4 If by Walborn.

3.2 The Grid of Standards and Calibration

The standards used are listed in Table 1 with references. The 'dagger' types listed by Morgan and Keenan [23] were used as primary standards. For stars of spectral classes earlier than O4, and luminosity classes for stars earlier than O9, for which the MK system does not have standards, those listed by Walborn [12] were used as primary standards.

All of Walborn's classification criteria for these spectral types were visible at our lower resolution. Standards taken from Garrison, Hiltner and Schild [27], Johnson and Morgan [22] and Walborn [26, 28] and spectral types from Hiltner, Garrison and Schild [29] were used for interpolation between the primary standards. In this reference frame, ζ Pup does look like an O4 I star, although it was the coolest of the O4's among the stars in our sample.

There are also some differences between Walborn's classifications and MK types among later spectral classes, mainly in that Walborn's types have more information; this is due to the use of different primary criteria, and/or of higher resolution that permits interpolations between half spectral classes. (ϵ Ori, for example is a B0 Ia MK standard, but it is a B0 Ia standard with moderate nitrogen deficiency according to Walborn). Our dispersion is the same as Walborn's but the resolution is poorer because of the image tube. So we cannot really distinguish between O9.5 and O9.7, for example, or B0 and B0.2; and since we are limited by our resolution and cannot interpolate between half spectral classes, or detect moderate line strength anomalies, we essentially use the MK standards. The classification, therefore is still on the MK system, with the possible exception of the very early type O stars.

It may be pointed out that while a higher dispersion may yield more information, in some cases it is far from desirable. The B2 V standard 22 Sco for example has a rotational velocity of 123 km/s; at dispersions of about 80Å/mm the rotational broadening is not noticeable. However, at higher dispersions as the broadening becomes apparent, the classification becomes more difficult. For

Table 1: The Classification Standards

Ia	Ib	II/III	IV/V
HD93129A O3 If* [12]			HDE303308 O3 V((f)) [12]
HD190429A O4 If^+ [12]			HD46223 O4 V((f)) [12], O4 [23]
		HD150136 O5 III [27]	HD46150 O5 [23], O5 V((f)) [12]
	HD69464 O6.5 Ib(f) [12]		
29 CMa O7 Ia [27]		ξ Per O7.5 III(n)((f)) [12], O7 III [27] HD93222 O7 III((f)) [12]	15 Mon O7 [23], O7 V((f)) [12]
HD151804 O8 Iaf [12]		λ Ori O8 III((f)) [12]	
HD148546 O9 Ia [27]	τ CMa O9 Ib [23]	ι Ori O9 III [23]	10 Lac O9 V [23] HR2806 O9 V [22], O9IV [28]
		HD189957 O9.5 III [12]	σ Ori O9.5 V [23]
ϵ Ori B0 Ia [23]		HD48434 B0 III [26],[22] HD108639 B0.2 III [28]	υ Ori B0 V [23] τ Sco B0 V [23]
κ Ori B0.5 Ia [23]	HR3090 B0.5 Ib [29]	ϵ Per B0.5 III [23] κ Aql B0.5 III [27],[22]	HD36960 B0.5 V [26]

(table con'd)

Table 1: Continued

Ia	Ib	II/III	IV/V
	ζ Per B1 Ib [23] HD109867 B0.7 Ib [28]	o Per B1 III [23] σ Sco B1 III [26]	ω Sco B1 V [23]
χ^2 Ori B2 Ia [23]	HR6743 B2 Ib [29]	γ Ori B2 III [23],[26]	22 Sco B2 V [23]
	3 Gem B2.5 Ib [23]		
o^2 CMa B3 Ia [23]		HR4074 B3 III [29]	
η CMa B5 Ia [23]	67 Oph B5 Ib [22]	τ Ori B5 III [27]	κ Hya B5 V ([27])
			19 Tau B6 IV [23]
		η Tau B7 III [23]	
β Ori B8 Ia [23]		27 Tau B8 III [23]	18 Tau B8 V [23]
			α Del B9 IV [23]
			α Lyr A0 V [23]
α Cyg A2 Ia [23]			
		o Sco A5 II [23]	
		θ^2 Tau A7 III [23]	

one thing, some (but not all) of the standards will themselves look different. Also, one has to consider wings when taking line ratios for temperature and luminosity classification of broadlined stars, and it is likely that the error in the two dimensional spectral type of a broadlined star is larger than that of a normal star.

The spectral atlases used were 'An Atlas of Representative Stellar Spectra '(Yamashita, Nariai, and Norimoto, 1978) [30] which uses spectrograms with a dispersion of 73 Å/mm ,covering the wavelength region between 3780Å and 4920Å and 'Revised MK Spectral Atlas for Stars Earlier than the Sun' (Morgan, Abt and Tapscott, 1978) [24] which uses spectrograms with a dispersion of 125 Å/mm, covering the spectral region between 3470Å and 4690Å. Our spectrograms cover the spectral interval from about 3750Å to a little beyond Hβ. The former [30] uses MK dagger types except for the O and early B stars, where priority is given to Walborn's types.

After looking at the spectral atlases to see which lines are useful in determining the temperature and luminosity types, the first step in the process of spectral classification is to study the spectra of the standard stars in order to choose those criteria that are useful for spectra obtained with our particular instrumental set up and, more importantly, to calibrate oneself. Each spectrogram is affected by intrinsic scatter in line strengths because only a fraction of the photons incident on the emulsion produce a darkening of the grains, and this number has statistical fluctuations. (If, using the same emulsion, under the same conditions, two exposures are taken of the same star, the spectra would look slightly different). The process of 'calibration' lies essentially in making up a mental picture of the point that the standard represents in the two dimensional system. This is done by taking into account, at each point, all the other standards, with the adjacent ones being given more weight. This process is like finding the 'best fit' to a set of points that define a curve, but are scattered about it. Consider for example, a single pair of lines that are temperature sensitive; if we look at the run of the ratio of their strengths against the spectral type, we expect a smooth curve; what we do get are points that are scattered about that curve. By studying the spectra of the standards one forms a mental picture of this curve, which in practice has to be determined for each pair of lines that appears in the spectrum.

3.3 Details of the Procedure

The spectra were first classified by comparing with the standards to get provisional spectral types. Then all the stars including the standards were arranged in order of decreasing temperature (or luminosity). The spectral types are thus checked for consistency, with each other as well as with the standards, since the spectra are arranged so that there is a continuous change in the line strengths. Once the stars were arranged in a sequence, the spectral type was decided by drawing cutoffs between the adjacent types, which of course were based on the standards. This method is particularly useful in picking out peculiarities.

An estimate of the accuracy of the assigned spectral types is provided by the following: there were two spectrograms (on different plates) of the star LSS 4161, of slightly different exposures. They were given the spectral types B1 Ib and B0.5 Ib without being aware that the same star was being classified twice. In assigning spectral types to stars, line strengths that are continuously and smoothly varying are used to put the star in a discrete class. So it is to be expected that there will be some error in classification since the spectrograms have scatter in line strengths, as was pointed out in section 3.2 and also due to exposure effects (which can be seen very clearly in the standard spectra, where several spectrograms of different exposures are recorded on a single plate); in the extreme cases, the wings tend to disappear in heavily exposed spectra and weak lines disappear in the very weakly exposed ones. The spectra are affected in varying degrees between these two extreme cases and this contributes to the error.

There is another effect that also arises from the non-linearity of the photographic emulsion's response curve. In the regions of the spectrograms that are under-exposed such that the continuum falls on the linear portion of the curve and the absorption line on the toe, the increased contrast between the line and the continuum causes the line to appear stronger. It is for these reasons that several exposures of different durations were taken of the standard stars. Other factors like plate defects are taken care of to a large extent by widening the spectrograms. Sometimes a feature is not uniform along the width of the spectrograms, indicating that the feature is not real, and may be due to flaws on the plate or some other unknown factors. The widening also increases the signal to noise by allowing one to 'integrate' along the width of the spectrogram.

The O3-O8 stars

For the stars of spectral types O3 to O8, the temperature and luminosity criteria are nearly orthogonal. Therefore all the stars, including the standards, were first arranged in a sequence of decreasing temperature (independent of the luminosity) using mainly the relative strengths of the He I

$\lambda 4471$ and He II $\lambda 4542$ lines. (The He I $\lambda 4471$/He II $\lambda 4542$ ratio is about 1 at O7). The He II $\lambda 4200$/He I+He II $\lambda 4026$ ratio was not found to be useful as a primary criterion. The He I $\lambda 3820$/He II $\lambda 3923$ lines were also used. The stars of each temperature class were then arranged in a sequence of decreasing luminosity using the criteria established by Walborn [26] for spectral classes O4 to O8: the strengths of the N III $\lambda\lambda 4634$-4642 emission and the He II $\lambda 4686$ emission/absorption. The absorption strengths of Si IV $\lambda 4089$ and and N III $\lambda 4097$ in O7 and O8 spectra and C III $\lambda\lambda 4068$-70 in the O8 spectra were also used as luminosity indicators. These lines were particularly useful when the spectra were not exposed well enough in the 4600Å region to rely entirely on the He II $\lambda 4686$ and N III $\lambda\lambda 4634$-42 lines. For the O3 stars the following criteria [25] were used: lines of He II $\lambda 4686$, N V $\lambda 4604$ and $\lambda 4620$ absorption and N IV $\lambda 4058$ emission.

O9 and later classes

For the stars of these classes the luminosity and temperature criteria are no longer orthogonal and spectral classification is an iterative process. The stars of each luminosity class (which had been determined during the first iteration) were arranged in a temperature sequence. The main temperature criteria are the ratio of He I $\lambda 4471$/He II $\lambda 4542$ for O9 and Si III $\lambda 4553$/Si IV $\lambda 4089$ in B0 and later types, in which He II is no longer present. The strength of O III $\lambda\lambda 3755$-3760 is also useful, but it has to be used with care since it is also sensitive to luminosity. The same is true of the ratio Si IV $\lambda 4116$/He I $\lambda 4121$ which is just resolved on these plates. The C III $\lambda 4267$ line was not found to be useful.

In classes Ia and Ib, He II $\lambda4542$ is present, and Si III absent at O9. Both He II $\lambda4542$ and Si III $\lambda4553$ are present, though very weakly at O9.5. He II is absent in B0. Si III starts to decrease with temperature after B1 Ib. The ratio of O II $\lambda4642$/C III $\lambda\lambda4647$-51 was useful in separating B0, B0.5 and B1. When Si IV has disappeared, at about B1, the ratio He I $\lambda4121/\lambda4144$ which decreases until it reaches zero at B3, is a good temperature criterion. In luminosity class III, Si III is absent in O9.5 but present in B0.

The lines of Si, C, N and O are all sensitive to luminosity, too. The luminosity classification is more difficult and is particularly so for the O9 stars. Si IV $\lambda4089$ does not show the expected change with luminosity at O9 possibly because it has a sharp maximum at this temperature class. τ CMa (O9 II std) has weaker Si IV $\lambda4089$ than ι Ori (O9 III std) while the He II $\lambda4686$ and C III lines are consistent with the luminosity classification. (He II $\lambda4542$ is weaker in τ CMa, so it may be cooler than the O9 III standard). It must also be kept in mind that τ CMa has been classified O9 II by Walborn; it was a O9 Ib MK dagger type standard but was replaced by 19 Cep in the atlas of Morgan, Abt and Tapscott [24]. Both τ CMa and ι Ori are known to be spectroscopic binaries, and some moderate spectral variability may also cause these discrepancies. There are similar problems with this line in the O9 III, IV and V standards. Si IV $\lambda4089$ has about the same strength in the O9 III, O9 IV and O9 V standards but the the strengths of He II $\lambda4686$ and C III $\lambda4068$ are consistent with the luminosity classification, as are the strengths of He I $\lambda4144$ and O III $\lambda3760$. Of the other luminosity criteria, He II $\lambda4686$/C III $\lambda4651$ and Si IV $\lambda4116$/He I $\lambda4121$, the first can be difficult because He II $\lambda4686$ is very weak except at class V. Si IV $\lambda4116$ and He I $\lambda4121$ are just resolved on the plates and can only be used to differentiate class I from classes III and V. All this makes it necessary to depend on C III $\lambda4068$ in some cases, but this can be complicated by anomalous line strengths. The strengths of He I $\lambda4388$, $\lambda4144$ and O III $\lambda3760$ are also useful, but again, are weak and temperature sensitive.

The MK spectral types of the program stars are given in Table 2 (the 'f' designation was retained in the spectral classification). The asterisk next to a star name indicates that there is a comment about the star in the text immediately following the table.

3.4 Peculiar Stars

As mentioned earlier, several peculiar stars were picked out. While some stars were noted as being decidedly peculiar, a tendency to label some as peculiar during the two-dimensional classification, even if the peculiarity was marginal and close to the noise level, must be admitted. It is for this reason that they were grouped together and checked for consistency later. They were grouped into sets of broadlined stars (with and without emission in the Balmer lines), and stars which had been noted as having strong C, N or O lines during the two-dimensional classification.

Two BN stars were found; they have very strong N lines for their type while C is weak or absent. From a non-LTE study of several OBN stars, which showed that He is also slightly enriched in these stars, Schönberner et al [31] have concluded that they are exposing processed matter at their surfaces, due to internal mixing or mass loss. Internal mixing can be caused by fast rotation of about 350 km/s. The stars studied by them have rotational velocities of only 100 to 190 km/s, so they suggest that the mixing might have ocurred at an earlier time after which the rotation slowed down. One of the two BN stars reported in Table 2, LSS 4103, has broad lines indicating a rotational velocity far greater than 250 km/s; it is only the second OBN star found to have broad lines (the other is HD 150574, ON9 III(n) [32]), and the only one with emission lines.

One star, LSS 4634, which is a post-asymptotic giant branch (post-AGB) object was found. Its spectrum is like that of a B9 supergiant; using this spectral type its distance was calculated to be 52 kpc. A search through the SIMBAD data base revealed that it had been observed by IRAS and had infrared colors of a planetary nebula [33]. This, along with its position (6.3 degrees below the Galactic plane), its photometric variability, and its spectral type, all indicate that this is a post-AGB object located at a much smaller distance (adopting $M_V = -3.5$ as a reasonable value for this class of objects [34], gives a distance of 5 kpc).

LSS 1160 was classified as a binary, possibly with a B1 III + B0 V spectrum. This star was noted as a suspected variable by Drilling [17]. It has been reported to be a β Lyrae type binary by Kilkenny et al [35]. They show that the colors correspond to a spectral class near B0, and luminosity class III or lower.

Some of the stars listed in Table 2 which have pronounced peculiarities have already been identified and studied. The helium stars listed here appear in the list compiled by Drilling and Hill [37]. The basic data on these stars (radial velocities, space distribution, position in the M_V—T_{eff} diagram) is given by Drilling [38].

The sdO stars listed in the table were included in the complete sample of 22 sdO stars studied by Drilling [39]. Their effective temperatures and absolute magnitudes placed them in the region of the H-R diagram crossed by all evolutionary tracks leading from the main sequence to the white dwarfs. Therefore this sample could be used to calculate the relative birth rates of various white dwarf progenitors—central stars of planetary nebulae, helium poor post-AGB stars, stars that evolved from the extended horizontal branch, and helium-rich post AGB stars—and it was concluded that most of the progenitors are central stars of planetary nebulae. One of these sdO object, LSS 2018, was found to be a double lined spectroscopic binary central star of a planetary nebula [40], and a photometric variable [36].

Two stars, LSS 3371 and LSS 1916 were found to be VV Cephei stars with very luminous blue components and are described by Drilling [41].

Table 2: The Spectral Types

	Star	Spectral Type		Star	Spectral Type
LSII	+12°3	O9 III	LSS	0477	B0 Ib
II	+14°8	B1 Vne_{2+}		0516	B0.5 III
II	+15°1	B3 $IIIne_1$		0552	O7 III
II	+16°8	B1 III		0606	B0.5 V(n)e2
II	+17°10	B1 III		0690	B1 III
II	+18°9 *	sdO		0695	B0 II
II	+20°13	O9.5 IV		0743	B1 II
II	+20°14	A1 Ia:		0810	B9 Iab
II	+22°7	F0 Ia?		0867	B0 V(n)e1
II	+33°5 *	He Star		0918 *	B1 $IIInne_2$
II	+39°53	O7 V:		1029	O7 IIInn
IV	+2°13 *	He Star		1046	B3 Ib
IV	+10°9 *	sdO		1096	B5 Iab
IV	-1°2 *	He Star		1106 *	B0.5 Vn
IV	-4°15	O6 Ib(f)		1108	B5 Ia
IV	-4°25	O9.5 Ia		1131	O7 V:n
IV	-8°11	B2 Ib(n)		1135	O6 III
IV	-8°28	O9.5 III		1148	O7 IIIn
IV	-12°1 *	sdO		1160 *	B1 IIIn
IV	-12°110	B1 Vn		1174	O9 V
IV	-13°15	O4 V		1205	O6 Ib(n)
IV	-14°109 *	He Star		1211	B0.5 Ib
VI	+2°11	B2 III		1215	O6 V
VI	+6°12 *	B2 $Vnne_{2+}$		1224	B3 III
VI	-1°5	B8 Ia		1253	B0.5 Vnn
LSS	0039	B0 Ibe2		1280	O9 III
	0070	B3 III		1288	B2 Ib
	0107	B1 III		1332	O9.5 Ib
	0218 *	B1 III		1397	B1 III:
	0271	B2 $IIIne_{2+}$		1408	B0.5 V
	0424	O7 Ia		1449	B2 III
	0453	B0 III		1467	B0.5 III
	0464	O9 III		1476	B2 III

(table con'd)

Table 2: Continued

	Star	Spectral Type		Star	Spectral Type
LSS	1484	B1 III	LSS	1878 *	O9.5 V
	1502	O7 IIIn		1880	O6 V
	1520 *	B1 Ia		1886	O4 V
	1542	O7 V		1887	O7 V(n)
	1565 *	B0.5 Ia		1892	O5 V
	1595 *	O9 Ia		1907	O5 II
	1614	O9.5 Ib		1912	B1 V
	1678	O9 III		1916 *	VV Cephi
	1683 *	B1 Vn		1922 *	He Star
	1704	B5 Ib		1938	O9 Ib
	1706	O7 III		1953	B3 III
	1740	B2.5 Ib		1972	O8 IIIn
	1778	B1 Vn		1976	B0.5 Ia
	1780A	B0 Ia		1982	B1 Ib
	1800	O6 V		1988	B0.5 Ib
	1807 *	B0 V(n)		2007	B0 Ib
	1808	B1 Ia		2018 *	sdO
	1809 *	O7 V		2025	O9 III
	1814 *	O6 V		2032	B3 Iab
	1819	O4 V		2049	B0.5 Ib
	1821	O9 V		2085	B5 Ia
	1847	O4 V		2089	O9 V
	1853	B1 Ib		2115	B0.5 Ia
	1854 *	B1 V		2241	B1 Ia
	1857	O9 III		2315	B1 Ia
	1860	O6 IIIn		2316	B1 Ia
	1864 *	B1 V		2318	B0.5 Ia
	1867	B0.5 V		2343	O7 III
	1869	O5 V		2352	O7 Ib
	1870	O9 III		2383 *	B2 IIIne$_{2+}$
	1871 *	O9.5 Vnne$_2$		2394 *	He Star
	1872	O9 V		2402	B2 V
	1874	O5 V		2436	B0 III

(table con'd)

Table 2: Continued

	Star	Spectral Type		Star	Spectral Type
LSS	2451A	B2 III	LSS	3159	B1 Ib
	2451B	B1 III		3171	B1 Ib
	2481	wd		3178	B0 III
	2513	B1 V		3181	O9 III(n)
	2526	B0.5 V		3183	O9.5 III
	2626	O6 V		3198	O5 IIIn
	2645	B0.5 III		3201	O7 IIIn
	2694	B1 V		3223	B0.5 Ia
	2695	O7 III		3236	B8 Ia
	2699	B3 Vn		3252	B2 III
	2702	O7 III		3259	O9.5 V
	2723	B0.5 Vne_1		3307	B0 Ia
	2751	B0.5 Ia		3332	O7 V:(n)
	2778	B1 Ib		3367 *	B1 Ia
	2800	B2 III		3371 *	VV Cephi
	2804 *	Dwarf Nova?		3378 *	He Star
	2824	B1 III		3390 *	B0 Ia
	2826 *	O7 III		3399	O9 Ia
	2854	B1 III(n)		3412 *	B1 Ia
	2863	B1 Ib		3426	B1 Ia
	2895	B1 III		3444A	O7 III
	2915	O7 Ib		3507	B0.5 Ia
	2983	B0.5 III		3514	B2 V
	3006	B2 Ib		3527	B0.5 Ia
	3052	B1 Ia		3528	B0 Ia
	3055 *	B0 Vn		3533	B0.5 Ia
	3058	B0 Ia^+		3639	B1.5 Ia
	3072	B2.5 Ia		3640	B3 III
	3094 *	B2 Ia		3672	O8II
	3135	O9 Ia		3711	O9.5 Ia:
	3139	B5 Ia		3730 *	B1 Ib:
	3140	O9.5 Ib		3740	O9.5 III
	3153	O7 III		3769	B0 Ia

(table con'd)

Table 2: Continued

	Star	Spectral Type		Star	Spectral Type
LSS	3780	B1 Ia^+	LSS	4161	B0.5 Ib
	3790	O9.5 Ia		4171	O6 Ib
	3799	O8 III:n		4200	O5 III
	3823	B0.5 III		4207	O4 III
	3868	O6 III		4239	B5 Ia
	3873	O5 III		4240	B1 Ia
	3874	O9.5 IV		4255	B8 Ia
	3894	B5 Ia		4293 *	B2 Ib
	3906	O7 V		4300 *	He Star
	3915 *	O7II		4304	O9.5 III
	3958 *	B0.5 III		4306N	O9.5 Ib
	3963	B3 Ia		4306S *	O9 V
	3968 *	B1.5 Iab		4309	O9 III
	3972	B1 Ib		4320	B0.5 Ia
	3976F	B3 V		4342	O9 III
	3976P	B1 III n?		4348	B0 Ia
	3978	B2 III		4351	B1 III
	3988	B0 Ia		4376	O8 III
	3997	B0 Ib		4379	B0.5 Ib(n)
	4009	B1 Ia		4391	B1 II
	4011	B0.5 Ib (n?)		4421	B1 III
	4015	B1II		4424	B2.5 IIIn
	4016	B1 Ib		4425	B0 Ia:e_{2+}
	4022	O9.5 III		4444	O8 III
	4032	B2 Ib		4482	B0.5 Ia
	4059	O5 V		4511	O9 III
	4103 *	BN0 IIIne_1		4537	B0.5 Ib
	4106	B2 Ib		4542	B0.5 Ia
	4121	B3 Iane_{2+}		4551	O9 Ib
	4129	B2.5 Ia		4561	B1 Ib
	4142	O3 III		4609	B0.5 V
	4145	B0.5 V		4614	B1 Ia
	4153	B0 III		4625 *	BN0 Ia

(table con'd)

Table 2: Continued

Star	Spectral Type	Star	Spectral Type
4634 *	B9 Ia^+e_{2+}	4957	B0 Ib
4665	O9 IIIn	4967	B0.5 Ia
4800	O7 III	4979	B1 Ia
4822	B1 V	4981	O9.5 V
4867	O9 V	5007 *	B0.5 Ia(n)
4872	B2 III	5019	O9 Ib
4880	O5 V	5026	B1 Ia
4896	B0 V(n)	5046	O7 II
4910	O7 II	5048	B1 III
4923 *	O9.5 IIInn	5083	O7 IIn
4925	O9 IV	5095	O9.5 III
4936	B2.5 $Ibne_1$	5099	B0.5 Ib
4939	B0.5 III	5128	B0.5 Ia
4955	B0.5 Ia		

LSII+18°9: Drilling [42]

LSII+20°14:A0Ia?

LSII+33°5: Drilling and Hill [37]

LSIV+2°13: Drilling and Hill [37]

LSIV+10°9: Drilling and Hill [37]

LSIV-1°2: Drilling and Hill [37]

LSIV-12°1: Drilling [42]

LSIV-14°109: Drilling and Hill [37]

LSVI+6°12: H-Poor?

0218: Sharp lines, O lines weak

0918: H-poor?; in a crowded field, and noted as a suspected variable by Drilling [17]

1106: CIII 4651 strong

1160: B1III+ B0V binary?; this was noted as a suspected variable by Drilling [17]. Kilkenny et al [35] find that it is a β Lyrae type variable.

1520: OII Strong?; noted as a suspected variable with a faint companion by Drilling [17].

1565: SiIII 4553 strong but not the other lines in multiplet

1595: NIII 4097 Strong

1683: Hγ core looks filled in; no emission in Hβ

1807: Nebular emission lines of [OIII], and in Hβ core

1809: Nebular emission lines of [OII], [OIII], and in Hβ, Hγ cores; noted as a suspected variable with a faint companion by Drilling [17].

1814: Nebular emission lines of [OIII]

1854: Nebular emission lines of [OII], [OIII], and in Hβ, Hγ cores

1864: Nebular emission lines of [OII], [OIII], and in Hβ, Hγ cores

1871: Nebular emission lines of [OIII], and in Hβ, Hγ cores

noted as a suspected variable by Drilling [17]. 1878: Nebular emission lines of [OII], [OIII], and in Hβ core

1916: Drilling [43]

1922: Drilling and Hill [37]

2018: Drilling [42]

2383: H-Poor?

2394: Drilling and Hill [37]

2804: Balmer lines have strong emission cores and broad, weak absorption wings. He I 4471 and 4713 in emission. Emission line at $\approx$5016$\AA$. Very faint emission in O II 4415 ?

2826: Strong NIII 4097?

3055: With strong CIII 4647 and OII 4642

3094: B2Ia$^+$?

3367: OII Strong suspected to be a variable by Drilling [17].

3371: Drilling [43]

3378: Drilling and Hill [37]

3390: Strong N III?

noted as a suspected variable by Drilling [?]

3412: CIII Strong

3730: Binary?

3915: Strong NIII 4097

3958: Strong CIII

3968: CIII strong??

4103: Very strong N lines, NIII 4511-15 present, and C lines absent

4293: CIII Strong?

4300: Drilling and Hill [37]

4306S: NIII Strong; C Weak??

4625: Very strong N lines, with C lines very weak

4634: Has been identified as a possible planetary nebula based on its IR colors [33]. This is not a massive B supergiant but a low-mass post-asymptotic giant branch star.

4923: Strong IS 4430

5007: ADS # 11310. A second spectrum taken the following night, shows emission lines, and was classified as B2Iane$_{2+}$; Hβ is in emission; Hγ has strong emission core; Hδ absent; higher Balmer lines very weak.

CHAPTER 4

THE SPACE DISTRIBUTION OF OB^+ STARS

4.1 Distribution of OB^+ Stars

Distribution projected onto the plane

The distances to the stars in Table 5 were calculated using the formula

$$V - M_V = 5\log d - 5 + R(E_{B-V}) \tag{4.1}$$

where the last term is the extinction in V magnitude, M_V is the absolute magnitude and V the apparent magnitude of the star, and E_{B-V} is the color excess. R is the ratio of extinction to reddening. The widely accepted value of $R = 3.2 \pm 0.2$ [8] was adopted for all directions. R is known to be remarkably uniform over the sky, although there are departures in some directions.

Spectral-type–absolute magnitude and spectral-type–intrinsic color calibrations were taken from Schmidt-Kaler [44]. These are shown in Tables 3 and 4, respectively. The calibrations were obtained by applying a smoothing function to contributions from several authors. For some intermediate spectral types, the magnitudes and intrinsic colors were obtained by interpolating between adjacent values.

In Table 5, spectral types, distances, galactic longitude, latitude, and color excess for nearly all OB^+ stars are shown. For stars that had published spectral types, column 2 gives the reference from which the type was taken.

Table 3: The Intrinsic Color Calibration

	Ia^+	I/Ia	Iab	Ib	II	III	IV	V
O3		-0.33				-0.33		-0.33
O4		-0.33				-0.33		-0.33
O5		-0.31			-0.32	-0.32		-0.33
O6		-0.31		-0.32		-0.32		-0.33
O7		-0.31		-0.31	-0.32	-0.32	-0.32	-0.32
O8		-0.29		-0.29	-0.31	-0.31		-0.32
O9		-0.27		-0.28	-0.31	-0.31	-0.31	-0.31
O9.5		-0.25		-0.26		-0.30	-0.30	-0.30
B0	-0.22	-0.23	-0.24	-0.29	-0.29	-0.29	-0.30	
B0.5		-0.21		-0.22		-0.28	-0.28	-0.28
B1	-0.19	-0.19		-0.20	-0.26	-0.26	-0.26	-0.26
B1.5		-0.18	-0.18	-0.19	-0.24	-0.25	-0.25	-0.25
B2		-0.16	-0.17	-0.18	-0.23	-0.24	-0.24	-0.24
B2.5		-0.14	-0.15	-0.16	-0.22	-0.22	-0.22	-0.22
B3		-0.12	-0.13	-0.14	-0.20	-0.20	-0.20	-0.20
B5		-0.08	-0.10	-0.10	-0.16	-0.17	-0.17	-0.17
B8		-0.02	-0.03	-0.04	-0.10	-0.11	-0.11	-0.11
B9	00.00	00.00	-0.02					

For the southern stars, these are mainly the spectral types from Drilling and Perry [45], Garrison et al [27], Humphreys [46], and others, in that order of preference. Unless otherwise mentioned, V and B-V were taken from Drilling [17, 18].

A plot of the distribution of the normal OB^+ stars in Table 5, projected onto the Galactic plane, is shown in Fig. 2. In the southern Milky Way, between $l = 220°$ and $l = 30°$, nearly all non-emission stars brighter than magnitude 12 are shown. In the northern Milky Way all the stars for which spectral types could be found in the literature, or which had unpublished

Table 4: The Absolute Magnitude Calibration

	Ia$^+$	I/Ia	Iab	Ib	II	III	IV	V
O3		-6.8				-6.8		-6.0
O4		-6.8				-6.5		-5.9
O5		-6.8			-6.6	-6.3		-5.7
O6		-6.8		-6.5		-6.1		-5.5
O7		-6.8		-6.3	-6.0	-5.9	-5.5	-5.2
O8		-6.8		-6.2	-6.0	-5.8		-4.9
O9		-6.8		-6.2	-5.9	-5.6	-5.2	-4.5
O9.5		-6.85		-6.15		-5.35	-4.95	-4.25
B0	-8.2	-6.9		-6.1	-5.7	-5.1	-4.7	-4.0
B0.5		-6.9		-5.95		-4.75	-4.25	-3.6
B1	-8.3	-6.9		-5.8	-5.4	-4.4	-3.8	-3.2
B1.5		-6.9	-6.4	-5.75	-5.1	-4.15	-3.45	-2.82
B2		-6.9	-6.4	-5.7	-4.8	-3.9	-3.1	-2.45
B2.5		-6.95	-6.35	-5.6	-4.65	-3.45	-2.75	-2.02
B3		-7.0	-6.3	-5.5	-4.5	-3.0	-2.4	-1.6
B5		-7.0	-6.2	-5.4	-4.0	-2.2	-1.7	-1.2
B8		-7.1	-6.2	-5.2	-3.1	-1.2	-0.7	-0.3
B9	-8.5	-7.1	-6.2					

spectral types from Drilling [47] are shown. The sun is at the center of the figure. The galactic longitude is marked in steps of 10°.

The figure includes nearly all the stars given in Table 5. Luminosity class V stars of spectral classes later than O9 are excluded because they could be less massive stars, of longer main sequence lifetimes, and therefore could well have moved away from the spiral arms. Also excluded are the subdwarfs, the He stars, dwarf nova and VV Cephei stars — all those stars that do not have an MK type in the table. The figure only covers a 10 kpc by 10 kpc box around the Sun, and 11 stars that are outside this box are not shown. Fig. 3 shows the distribution of all O3 to O8 stars, and supergiants of later

Table 5: Distances to OB^+ Stars

LSS	Sp. Type	Ref	l(°)	b(°)	V	B-V	E_{B-V}	d(pc)
70	B3 III		195.25	3.34	11.58	0.15	0.35	4900
107	B1 III		228.41	-6.42	10.86	0.28	0.54	5100
122	B1 Ib		222.17	-2.16	6.47	0.19	0.39	1600
218	B1 III		230.75	-3.80	10.37	0.36	0.62	3600
271	B2 IIIne$_{2+}$		233.92	-4.31	10.43	0.23	0.47	3700
352	B1 VNEP	[27]	239.54	-5.23	7.18	-0.09	0.17	900
385	B1 Ib-II	[27]	235.52	-2.47	6.79	0.10	0.30	2100
424	O7 Ia		230.74	0.86	9.48	0.48	0.79	5600
453	B0 III		230.63	1.50	10.67	0.50	0.79	4450
464	O9 III		230.70	1.63	10.40	0.62	0.93	4000
477	B0 Ib		234.20	-0.19	8.97	0.50	0.74	3500
516	B0.5 III		231.40	1.95	10.79	0.31	0.59	5400
528	O9 IV	[27]	242.68	-4.30	8.15	0.01	0.32	2900
538	O9 Ib	[27]	242.43	-4.03	8.42	0.33	0.61	3400
552	O7 III		232.31	1.94	10.57	0.25	0.57	8500
606	B0.5 Vne$_2$		239.37	-1.16	10.43	0.34	0.62	2600
640	B3 Iab	[27]	247.12	-5.07	7.65	0.53	0.66	2300
690	B1 III		249.30	-5.68	10.51	0.48	0.74	3200
695	B0 II		248.96	-5.36	10.98	0.96	1.25	3400
716	B2 IIIne	[27]	242.72	-1.39	9.21	0.14	0.38	2400
719	B3 Ia	[27]	248.16	-4.54	8.84	1.09	1.21	2500
743	B1 II		247.95	-4.16	10.95	0.82	1.08	3800
810	B9 Iab		248.15	-3.35	10.54	1.08	1.10	4400
840	O6.5 IIIf	[27]	243.82	0.14	9.69	0.37	0.69	5000
846	O4 V((f))	[27]	243.14	0.71	9.37	0.08	0.41	6200
867	B0 V(n)e$_1$		246.23	-0.61	10.78	0.41	0.71	3200
870	O6 Iafp	[27]	245.45	-0.10	9.99	0.17	0.48	11200
876	B0.5 IIIne	[27]	246.19	-0.40	9.76	0.23	0.51	3800
918	B1 IIInn		247.64	-0.46	10.90	0.41	0.67	4300
1007	O7 III	[27]	252.40	-0.04	9.27	0.33	0.65	4200
1022	O7 III(f)	[27]	253.61	-0.30	8.80	0.29	0.61	3500
1029	O7 IIInn		253.71	-0.09	10.51	0.62	0.94	4800
1034	B0.7 Ib	[27]	259.50	-3.91	7.21	0.29	0.50	2000
1046	B3 Ib		252.33	1.54	11.23	0.34	0.48	10900
1061	O9 Ib(f)	[27]	261.76	-3.77	8.27	0.52	0.80	2400
1082	B0 V:nne	[27]	260.77	-2.20	6.22	-0.05	0.25	800
1096	B5 Iab		264.76	-4.17	10.52	0.44	0.54	10000
1106	B0.5 Vn		262.53	-1.46	10.58	0.63	0.91	1800
1108	B5 Ia		263.78	-2.27	9.80	0.97	1.05	4900
1116	O8.5 Ib(f)	[27]	264.04	-1.95	7.55	0.22	0.50	2700

(table con'd)

Table 5: Continued

LSS	Sp. Type	Rcf	l(°)	b(°)	V	B-V	E_{B-V}	d(pc)
1126	B1.5 III	[27]	266.23	-3.38	8.96	0.27	0.52	1900
1131	O7 V:n		265.18	-2.26	10.74	0.50	0.82	4600
1135	O6 III		265.20	-2.18	10.88	0.38	0.70	8900
1148	O7 IIIn		265.29	-1.95	7.53	0.02	0.34	2900
1154	O8 II	[27]	263.96	-0.47	7.53	0.39	0.70	1800
1155	B0 Ia	[27]	258.29	4.18	7.40	0.38	0.61	2900
1157	B1 IIp	[27]	265.86	-1.90	7.87	0.01	0.27	3000
1160	B1 IIIn		264.71	-0.80	10.01	1.03	1.29	1100
1165	B1 Ib	[27]	267.01	-2.56	7.83	0.36	0.56	2300
1167	B1 IVe	[27]	266.87	-2.29	8.23	0.19	0.45	1300
1172	O9.5 Ib	[53]	264.69	-0.37	9.42	0.70	0.96	3200
1174	O9 V		263.61	0.55	10.63	0.66	0.97	2500
1184	B1.5 Iabp	[27]	264.14	0.27	7.59	0.73	0.91	1600
1198	O9 Ib	[27]	263.53	1.52	7.16	0.30	0.58	2000
1204	O6 IIIn(f)	[27]	267.58	-1.63	8.20	0.40	0.72	2500
1205	O6 Ib(n)		263.02	2.30	9.81	0.70	1.02	4100
1211	B0.5 Ib		266.46	-0.31	10.00	1.02	1.24	2500
1214	O9.5 Iab	[27]	270.23	-3.37	7.07	0.13	0.38	2900
1215	O6 V		268.00	-1.38	10.24	0.88	1.21	2400
1216	O5 If	[27]	267.98	-1.36	8.39	0.89	1.20	1900
1224	B3 III		269.20	-1.90	10.44	0.87	1.07	1000
1227	B0.5 Iae	[27]	263.06	3.93	6.89	0.48	0.69	2100
1242	O9.5 Ia	[55]	268.89	-0.38	8.98	1.12	1.37	1946
1248	B1 IIIe	[27]	272.73	-3.31	8.91	0.39	0.65	1800
1253	B0.5 Vnn		269.34	0.25	10.44	1.10	1.38	840
1255	B5 Ia	[27]	267.36	2.25	4.96	0.21	0.29	1600
1268	B2 $Ia^{+}e$	[27]	271.63	-0.67	7.55	1.34	1.49	1600
1280	O9 III		275.07	-2.84	11.27	0.42	0.73	8100
1285	O9 Ia	[27]	272.07	0.44	9.37	1.13	1.40	2200
1288	B2 Ib		271.97	0.68	10.20	1.03	1.21	2500
1322	B1 III:ne	[27]	271.43	3.62	9.31	0.27	0.53	2500
1332	O9.5 Ib		272.69	3.53	10.44	0.56	0.82	6200
1397	B1 III:		279.60	1.24	11.50	0.60	0.86	4300
1408	B0.5 V		283.82	-4.21	11.61	0.03	0.31	7000
1449	B2 III		280.35	2.77	11.82	0.13	0.37	8100
1467	B0.5 III		279.69	4.45	7.98	-0.05	0.23	2500
1476	B2 III		284.94	-3.23	11.69	0.30	0.54	5900
1484	B1 III		284.05	-1.54	11.39	0.75	1.01	3250
1502	O7 IIIn		284.91	-2.18	10.39	0.43	0.75	6000
1520	B1 Ia		284.55	-1.11	10.25	0.74	0.93	6800

(table con'd)

Table 5: Continued

LSS	Sp. Type	Ref	l(°)	b(°)	V	B-V	E_{B-V}	d(pc)
1524	B1 IIIn	[27]	284.30	-0.60	9.02	0.23	0.49	2300
1542	O7 V		285.67	-2.36	10.23	0.09	0.41	6700
1562	O7 IIf	[27]	285.88	-2.41	9.40	0.18	0.50	5800
1565	B0.5 Ia		284.62	-0.29	11.04	0.89	1.10	7700
1583	B0.5 III	[27]	284.62	0.02	9.62	0.15	0.43	4000
1595	O9 Ia		285.35	-1.08	10.08	0.47	0.74	8000
1614	O9.5 Ib		286.05	-1.66	10.03	0.82	1.08	3500
1639	B1 IIIne	[27]	286.86	-2.37	9.69	0.13	0.39	3700
1678	O9 III		286.82	-1.59	9.79	0.01	0.32	7500
1683	B1 Vn		285.89	0.08	10.32	0.00	0.26	3400
1704	B5 Ib		286.89	-1.17	11.33	0.39	0.49	10800
1706	O7 III		285.75	0.94	10.47	0.45	0.77	6000
1722	B0 Ia	[46]	288.14	-3.14	10.21	0.41	0.64	10300
1726	B0.5 Iab	[46]	286.38	0.19	9.88	0.59	0.80	5500
1740	B2.5 Ib		286.11	0.84	10.92	0.76	0.92	5200
1778	B1 Vn		287.02	-0.32	10.59	0.09	0.35	3400
1780A	B0 Ia		287.41	-1.05	9.59	0.53	0.76	6500
1800	O6 V		287.41	-0.79	9.65	0.28	0.61	4400
1807	B0 V(n)		287.33	-0.55	9.97	0.33	0.63	2500
1808	B1 Ia		287.38	-0.63	10.07	0.52	0.71	8700
1809	O7 V		287.40	-0.64	10.98	0.55	0.87	4800
1814	O6 V		287.39	-0.59	9.61	0.32	0.65	4000
1819	O4 V		287.41	-0.58	8.74	0.23	0.56	3700
1821	O9 V		287.67	-1.05	9.33	0.00	0.31	3700
1847	O4 V		287.57	-0.71	8.44	0.09	0.42	4000
1853	B1 Ib		287.65	-0.85	9.50	0.78	0.98	2700
1854	B1 V		287.56	-0.66	10.71	0.26	0.52	2800
1857	O9 III		287.41	-0.36	8.37	0.13	0.44	3300
1860	O6 IIIn		287.67	-0.85	9.32	0.24	0.56	5300
1864	B1 V		287.69	-0.86	11.11	0.19	0.45	3700
1867	B0.5 V		288.02	-1.45	11.23	0.48	0.76	3000
1869	O5 V		287.59	-0.61	8.15	0.15	0.48	2900
1870	O9 III		287.63	-0.68	9.93	0.38	0.69	4600
1871	O9.5 Vnn_2		287.60	-0.62	9.58	0.14	0.44	3050
1872	O9 V		287.64	-0.67	9.26	0.25	0.56	2500
1874	O5 V		287.64	-0.65	9.24	0.33	0.66	3700
1878	O9.5 V		287.64	-0.64	10.03	0.18	0.48	3500
1880	O6 V		287.78	-0.84	10.20	0.36	0.69	5000
1886	O4 V		287.79	-0.71	10.04	0.70	1.03	3400
1887	O7 V(n)		287.25	0.35	10.70	0.56	0.88	4100

(table con'd)

Table 5: Continued

LSS	Sp. Type	Ref	l(°)	b(°)	V	B-V	E_{B-V}	d(pc)
1892	O5 V		287.84	-0.73	10.41	0.56	0.89	4500
1894	O9.5 III	[46]	288.16	-1.33	9.74	0.35	0.65	4000
1900	B1 III:nne	[27]	285.58	3.79	9.35	-0.04	0.22	4100
1907	O5 II		288.03	-0.87	8.38	0.31	0.63	3900
1912	B1 V		287.75	-0.30	10.69	0.32	0.58	2500
1935	B1 Ia	[27]	287.92	-0.19	7.72	0.44	0.63	3300
1938	O9 Ib		288.50	-1.33	10.43	0.27	0.55	9400
1939	B0.7 Iab	[27]	287.69	0.31	9.00	0.74	0.94	3000
1953	B3 III		287.53	0.89	10.76	0.61	0.81	1700
1972	O8 IIIn		288.90	-1.50	9.94	0.13	0.44	7400
1973	B1 Ib	[27]	288.33	-0.32	7.78	0.37	0.57	2200
1976	B0.5 Ia		288.40	-0.40	10.44	0.40	0.61	12000
1982	B1 Ib		287.88	0.78	10.97	0.52	0.72	7800
1988	B0.5 Ib		288.38	-0.15	10.45	0.55	0.77	6100
2007	B0 Ib		288.62	-0.31	10.33	0.46	0.70	6900
2025	O9 III		288.29	0.80	9.82	0.26	0.57	5200
2032	B3 Iab		289.06	-0.52	10.51	0.35	0.48	11300
2049	B0.5 Ib		289.03	-0.19	10.74	0.29	0.51	10300
2078	B0.5 Iab	[27]	289.17	0.50	8.84	0.43	0.64	4300
2085	B5 Ia		289.14	0.81	10.62	0.85	0.93	8500
2089	O9 V		289.69	-0.30	11.28	0.43	0.74	4800
2115	B0.5 Ia		290.42	-1.55	10.48	0.77	0.98	7100
2183	O8.5 Ib(f)	[27]	289.28	3.06	7.09	0.08	0.36	2700
2241	B1 Ia		295.35	-10.58	10.07	0.08	0.27	16600
2315	B1 Ia		292.57	-1.00	10.46	0.61	0.80	9100
2316	B1 Ia		291.89	1.07	10.02	0.58	0.77	7800
2318	B0.5 Ia		292.58	-0.77	10.94	0.72	0.93	9400
2343	O7 III		293.19	-0.75	11.14	0.74	1.06	5400
2352	O7 Ib		293.50	-1.04	10.00	0.64	0.95	4500
2383	B2 IIIne$_{2+}$		293.45	0.61	11.32	0.30	0.54	5000
2384	O9 Ib	[27]	294.35	-2.09	8.43	0.21	0.49	4100
2402	B2 V		294.11	-0.03	9.23	0.01	0.25	1500
2436	B0 III		294.92	-1.44	10.91	0.67	0.96	3900
2451A	B2 III		294.96	-0.82	10.55	0.40	0.64	3000
2451B	B1 III		294.96	-0.82	10.86	0.43	0.69	4100
2461	B1:III:nne	[27]	294.42	1.75	9.72	0.17	0.43	3500
2513	B1 V		296.49	-2.77	11.39	0.45	0.71	2900
2526	B0.5 V		296.31	-0.37	10.84	0.16	0.44	4000
2572	B0 Ia	[27]	296.51	4.02	9.25	0.38	0.61	6900
2626	O6 V		298.41	2.23	10.42	0.37	0.70	5400

(table con'd)

Table 5: Continued

LSS	Sp. Type	Ref	l(°)	b(°)	V	B-V	E_{B-V}	d(pc)
2628	O9.5 Ia	[27]	298.67	1.25	9.45	0.64	0.89	4900
2636	B1 IIIne	[27]	299.20	-1.90	8.52	0.10	0.36	2300
2645	B0.5 III		299.88	-4.36	8.97	1.28	1.56	560
2674	B0.5 Iab	[27]	299.97	0.48	8.71	0.38	0.59	4400
2694	B1 V		300.38	1.46	11.84	0.37	0.63	4000
2695	O7 III		300.49	0.29	10.46	0.71	1.03	4100
2699	B3 Vn		300.87	-2.40	11.03	0.93	1.13	600
2702	O7 III		300.68	1.08	11.23	0.58	0.90	7100
2720	B1 Ib	[27]	301.71	-4.35	6.28	0.05	0.25	1800
2723	B0.5 Vne		301.43	2.38	10.00	0.12	0.40	2900
2726	O8 III	[27]	301.57	0.41	8.83	0.39	0.70	3000
2751	B0.5 Ia		302.25	-2.22	11.21	0.74	0.95	10300
2778	B1 Ib		302.79	0.13	10.56	1.07	1.27	2880
2800	B2 III		303.16	2.46	9.81	0.14	0.38	3150
2814	B0.5 IVn	[84]	303.23	2.49	9.44	0.14	0.42	2900
2824	B1 III		303.33	-3.51	11.82	0.30	0.56	7700
2826	O7 III		303.39	1.30	10.69	1.09	1.41	2600
2834	B0.5 Ia	[27]	303.49	-1.49	7.36	0.80	1.01	1606
2854	B1 III(n)		303.91	1.22	10.62	1.17	1.43	1200
2863	B1 Ib		303.99	1.19	10.34	1.24	1.44	2000
2895	B1 III		304.47	1.52	10.46	1.18	1.44	1100
2914	O9 Ib	[27]	304.52	-1.42	8.63	0.43	0.71	3200
2915	O7 Ib		304.67	1.46	9.88	1.19	1.50	1900
2946	B0.5 Iab	[27]	305.00	-0.07	8.57	0.56	0.77	3200
2949	B1 IIIne	[27]	304.54	-8.00	8.48	0.08	0.34	2300
2958	B1 Ia	[27]	305.40	3.03	7.99	0.52	0.71	3300
2983	B0.5 III		305.64	1.58	10.50	0.73	1.01	2500
2995	B1 Ia	[27]	305.79	0.87	9.04	0.76	0.95	3800
3000	B1 IIIne	[27]	305.86	0.97	9.78	0.28	0.54	3100
3006	B2 Ib		305.73	-1.20	11.00	0.88	1.06	4600
3014	B1 Ia	[27]	305.88	-0.97	7.79	0.60	0.79	2700
3038	B0.5 Ia	[27]	307.08	6.83	6.06	0.28	0.49	1900
3052	B1 Ia		306.58	0.21	10.13	0.83	1.02	5700
3055	B0 Vn		306.53	-0.49	11.69	0.37	0.67	5100
3058	B0 Ia+		306.55	-1.04	10.49	0.73	0.95	13500
3072	B2.5 Ia		307.02	0.54	9.70	1.31	1.45	2500
3094	B2 Ia		307.14	-0.95	10.65	0.91	1.07	6700
3135	O9 Ia		308.10	-1.39	10.93	0.84	1.11	6800
3139	B5 Ia		308.50	0.17	9.59	1.22	1.30	3100
3140	O9.5 Ib		308.24	-1.29	10.32	0.89	1.15	3600

(table con'd)

Table 5: Continued

LSS	Sp. Type	Ref	l(°)	b(°)	V	B-V	E_{B-V}	d(pc)
3153	O7 III		309.13	-0.20	10.70	0.70	1.02	4600
3159	B1 Ib		309.22	-0.54	10.28	0.52	0.72	5700
3170	O8 IIInep	[27]	309.91	-0.68	8.14	0.06	0.37	3600
3171	B1 Ib		309.56	-2.40	10.44	0.64	0.84	5100
3178	B0 III		309.42	-5.49	10.45	0.09	0.38	7400
3181	O9 III(n)		310.72	-0.75	11.05	0.92	1.23	3500
3183	O9.5 IIIn		310.18	-3.14	11.37	0.38	0.68	8100
3193	B1 III:e	[27]	311.35	-0.85	8.98	0.34	0.60	2000
3194	B1:Vnne	[27]	311.33	-0.93	9.22	0.34	0.60	1300
3198	O5 IIIn		310.68	-3.77	10.62	0.30	0.62	9700
3199	ON9 Ia	[27]	311.02	-2.80	8.83	0.38	0.65	5100
3201	O7 IIIn		311.16	-2.57	10.29	0.37	0.69	6300
3223	B0.5 Ia		312.86	-1.67	10.69	0.63	0.84	9600
3236	B8 Ia		315.38	3.45	9.92	1.28	1.30	3700
3252	B2 III		314.66	-0.12	10.26	0.35	0.59	2800
3259	O9.5 V		312.78	-5.40	10.82	0.13	0.43	5500
3280	O9 III	[45]	316.76	0.02	10.72	0.68	0.99	4300
3283	O6 III	[45]	318.18	1.78	10.31	1.00	1.32	2700
3298	O6 III	[45]	319.27	0.66	10.24	0.87	1.19	3200
3307	B0 Ia		317 23	-4.64	9.51	1.18	1.41	2400
3313	O9.5 Ib	[45]	321.07	0.96	10.13	1.20	1.46	2100
3314	O9.5 Ia	[45]	320.72	0.26	10.31	1.23	1.48	3100
3318	B1 Ia	[45]	321.19	0.56	10.13	1.73	1.92	1500
3327	O9.5 Vn	[52]	320.51	-1.20	11.30	0.90	1.20	2200
3328	B1.5 Ib	[27]	320.52	-1.20	8.13	1.01	1.20	1100
3332	O7 V:(n)		318.84	-4.58	11.32	0.94	1.26	3100
3339	B1.5 Ve	[27]	319.32	-4.21	9.78	0.52	0.77	1100
3341	B0 Ib	[45]	326.31	6.79	10.45	0.39	0.63	8100
3345	B1.5 Ia	[27]	321.22	-1.76	7.81	0.99	1.17	1600
3349	B0.5 IVn	[27]	318.99	-5.65	9.75	0.19	0.47	3200
3367	B1 Ia		322.69	-2.13	8.71	2.05	2.24	500
3372	O9 Ia	[45]	323.10	-2.26	10.44	0.68	0.95	6900
3386	O4 III	[45]	326.31	0.74	10.91	1.61	1.94	1700
3388	B0.5 III	[45]	323.11	-3.71	12.05	0.47	0.75	7600
3390	B0 Ia		324.70	-2.09	10.40	1.09	1.32	4100
3399	O9 Ia		330.42	4.59	10.46	0.64	0.91	7400
3412	B1 Ia		330.62	3.80	10.30	1.15	1.34	3800
3426	B1 Ia		328.04	-0.49	10.49	1.24	1.43	3650
3439	B1.5 Ia	[27]	325.31	-4.27	7.05	0.20	0.38	3500
3443	O5 III	[45]	328.22	-1.03	10.94	1.10	1.42	3500

(table con'd)

Table 5: Continued

LSS	Sp. Type	Ref	l(°)	b(°)	V	B-V	E_{B-V}	d(pc)
3444A	O7 III		328.56	-0.72	9.85	0.95	1.27	2200
3449	B2:III:nne	[45]	328.15	-1.58	11.33	0.63	0.87	3100
3452	B1.5 V	[27]	324.55	-5.97	7.29	-0.02	0.23	750
3455	B0 Ib	[45]	328.01	-2.22	10.47	0.74	0.98	4900
3462	O9 III	[45]	329.05	-1.57	10.52	0.99	1.30	2500
3491	B0.7 Ia	[27]	333.18	2.01	8.27	0.94	1.14	2000
3507	B0.5 Ia		336.13	4.72	10.10	1.03	1.24	4000
3514	B2 V		331.90	-0.15	10.51	0.34	0.58	1700
3515	B0.5:Ia:	[45]	331.28	-0.88	11.39	1.17	1.38	6000
3521	B0.5 Ia	[45]	331.35	-0.94	10.38	0.93	1.14	5300
3527	B0.5 Ia		331.64	-0.98	9.86	0.85	1.06	4700
3528	B0 Ia		331.55	-1.07	9.80	0.84	1.07	4500
3530	B0.5 Ia	[45]	331.70	-0.96	9.84	0.91	1.12	4300
3533	B0.5 Ia		331.89	-0.87	9.87	0.89	1.10	4500
3539	O6 IIIn	[45]	331.86	-1.08	10.71	0.79	1.11	4500
3562	B0.5 Ia	[56]	331.44	-2.20	8.54	0.55	0.76	4000
3564	B2 III	[45]	333.88	0.28	10.47	0.78	1.02	1700
3573	B1 Ia	[45]	331.74	-2.07	7.73	0.35	0.54	3800
3579	B1 Ia	[45]	337.28	3.42	10.37	1.02	1.21	4800
3603	B0 Ia	[45]	334.43	-0.18	9.77	0.77	1.00	4900
3618	O6 III	[45]	332.72	-2.65	10.26	0.72	1.04	4000
3620	B0.5 Ia	[45]	333.50	-1.89	9.17	0.55	0.76	5300
3625	B1.5 Ia	[27]	337.25	1.58	5.38	0.56	0.74	960
3639	B1.5 Ia		342.47	5.86	10.93	0.84	1.02	8200
3640	B3 III		335.22	-1.09	9.88	0.81	1.01	850
3650	B0.7 Ia	[27]	335.83	-0.77	8.81	0.61	0.81	4200
3653	O7 V	[45]	335.30	-1.32	10.90	0.68	1.00	3800
3672	O8 II		340.54	3.00	5.47	0.39	0.70	700
3689	O9.5 Ia	[45]	334.87	-2.73	11.08	1.06	1.31	5600
3702	B0 IV	[45]	336.72	-1.57	8.48	0.18	0.47	2200
3707	O9 Ib	[56]	337.66	-0.82	9.53	0.41	0.69	5100
3711	O9.5 Ia:		340.31	1.33	10.29	0.64	0.89	7200
3716	O9 Ib	[27]	339.46	0.30	9.46	0.64	0.92	3500
3718	B1 Ib:n	[27]	337.93	-1.07	9.68	0.31	0.51	5900
3730	B1 Ib:		340.38	0.84	10.40	1.45	1.65	1500
3740	O9.5 III		338.56	-1.14	9.22	0.40	0.70	2900
3741	O6.5 If	[27]	338.56	-1.15	7.29	0.34	0.65	2500
3746	O9 Ia	[27]	339.51	-0.41	8.74	0.62	0.89	3500
3769	B0 Ia		338.92	-1.69	9.87	0.82	1.05	4800
3780	B1 Ia+		344.76	2.91	8.84	0.77	0.96	6500

(table con'd)

Table 5: Continued

LSS	Sp. Type	Ref	l(°)	b(°)	V	B-V	E_{B-V}	d(pc)
3782	B1 Ia	[45]	338.30	-2.58	8.65	0.78	0.97	3100
3790	O9.5 Ia		343.33	1.41	7.04	0.39	0.64	2300
3799	O8 III:n		340.73	-0.97	11.04	0.89	1.20	4000
3823	B0.5 III		341.91	-0.26	10.23	0.71	0.99	2300
3868	O6 III		345.13	1.53	10.25	0.79	1.11	3600
3873	O5 III		345.26	1.47	10.10	0.85	1.17	3400
3874	O9.5 IV		345.14	1.36	10.07	1.00	1.30	1500
3894	B5 Ia		344.68	0.03	9.45	1.49	1.57	1900
3903	B1 Ib	[27]	340.57	-3.62	7.10	0.63	0.83	1100
3906	O7 V		345.01	-0.30	10.60	0.99	1.31	2100
3907	B2:III:ne	[45]	341.12	-3.33	10.87	0.77	1.01	2000
3908	B0.5 IIIn	[27]	356.16	8.26	8.80	0.09	0.37	3000
3915	O7 II		345.24	-0.34	11.23	0.87	1.19	4800
3928	B1:IIInne	[27]	341.06	-4.22	6.94	0.39	0.65	1600
3958	B0.5 III		349.49	1.42	11.12	1.08	1.36	2000
3963	B3 Ia		346.54	-0.88	9.95	1.57	1.69	2000
3968	B1.5 Iab		347.16	-0.51	10.49	0.91	1.09	4800
3972	B1 Ib		347.18	-0.53	10.72	0.94	1.14	3750
3976F	B3 V		347.29	-0.47	10.90	0.58	0.78	1000
3976P	B1 IIIn?		347.29	-0.47	10.96	0.78	1.04	2550
3978	B2 III		359.95	8.69	12.46	0.36	0.60	7700
3988	B0 Ia		347.27	-0.86	10.82	0.99	1.22	5800
3997	B0 Ib		347.73	-0.69	10.26	1.33	1.57	1850
4009	B1 Ia		347.70	-0.88	10.56	0.89	1.08	6300
4011	B0.5 Ib(n?)		347.70	-0.91	10.62	1.01	1.23	3400
4015	B1 II		348.82	-0.16	10.41	1.01	1.27	2200
4016	B1 Ib		347.35	-1.25	10.58	0.90	1.10	3700
4022	O9.5 III		348.67	-0.36	10.39	0.85	1.15	2600
4032	B2 Ib		347.53	-1.30	10.93	0.87	1.05	4500
4044	O9.5 Iab	[27]	357.57	5.82	7.95	0.51	0.76	2500
4056	O6 III	[45]	348.94	-0.51	10.01	0.81	1.13	3200
4059	O5 V		349.89	0.12	9.76	0.91	1.24	2000
4083	B0.5 III	[27]	342.94	-5.15	7.38	0.21	0.49	1300
4103	BN0 IIIne$_1$		349.65	-0.67	9.72	1.10	1.39	1200
4106	B2 Ib		349.67	-0.71	11.04	0.85	1.03	4900
4111	B0.5 IIIne	[45]	349.60	-0.89	11.08	0.76	1.04	3200
4120	B3 Iap	[27]	349.95	-0.79	6.32	0.77	0.89	1200
4121	B3 Iane$_{2+}$		348.96	-1.57	9.24	1.07	1.19	3100
4126	O7 IIIn	[45]	351.34	-0.06	11.06	0.97	1.29	3700
4129	B2.5 Ia		350.65	-0.64	9.81	1.41	1.55	2300

(table con'd)

Table 5: Continued

LSS	Sp. Type	Ref	l(°)	b(°)	V	B-V	E_{B-V}	d(pc)
4142	O3 III		353.17	0.90	10.40	1.54	1.87	1750
4143	B0 Ia	[27]	350.25	-1.15	9.24	0.84	1.07	3500
4145	B0.5 V		350.29	-1.14	10.58	0.87	1.15	1300
4153	B0 III		350.59	-1.14	10.42	1.06	1.35	1700
4161	B0.5 Ib		357.96	3.67	10.11	0.81	1.03	3600
4171	O6 Ib		352.15	-0.54	9.95	1.22	1.54	2000
4177	O6 Vn	[45]	353.30	0.08	10.08	1.12	1.45	1500
4200	O5 III		357.81	2.14	10.57	0.85	1.17	4200
4207	O4 III		354.80	-0.10	10.12	0.92	1.25	3300
4210	B5 Ib	[27]	357.94	1.94	7.21	0.37	0.47	1700
4237	B0.5 Ia	[45]	354.79	-0.72	8.45	0.97	1.18	2100
4239	B5 Ia		354.63	-0.83	9.97	1.42	1.50	2700
4240	B1 Ia		355.02	-0.57	10.70	0.98	1.17	5900
4254	B1 Ia	[51]	354.73	-0.93	9.27	1.12	1.31	2500
4255	B8 Ia		355.08	-0.70	8.82	1.59	1.61	1400
4258	B0.5 Ia	[54]	355.23	-0.62	8.41	0.80	1.01	2600
4266	B0.5 Ib	[45]	355.10	-0.75	10.04	1.42	1.64	1400
4293	B2 Ib		352.88	-2.48	11.39	0.83	1.01	5900
4298	B2 II	[45]	352.89	-2.51	11.09	0.82	1.05	3200
4304	O9.5 III		355.08	-1.21	10.40	0.84	1.14	2600
4306N	O9.5 Ib		358.58	1.31	9.52	0.74	1.00	3100
4306S	O9 V		358.58	1.31	9.72	0.66	0.97	1700
4309	O9 III		354.14	-1.91	10.47	0.94	1.25	2600
4314	O9.5 Iab	[27]	355.32	-1.36	8.60	0.96	1.21	1700
4320	B0.5 Ia		353.27	-2.76	10.84	0.90	1.11	6900
4342	O9 III		3.60	3.02	9.89	0.64	0.95	3100
4348	B0 Ia		358.90	-0.22	10.34	1.38	1.61	2600
4351	B1 III		358.59	-0.63	10.83	0.98	1.24	1800
4352	O9.5 Iab	[54]	0.53	0.58	9.37	1.38	1.63	1300
4356	B1:III:nne	[27]	1.36	1.05	8.43	0.44	0.70	1300
4359	B0.5 Ib	[51]	359.09	-0.43	10.74	1.06	1.28	3300
4376	O8 III		4.19	2.41	10.73	0.82	1.13	3800
4379	B0.5 Ib(n)		2.65	1.43	10.69	0.84	1.06	4500
4386	B3 Ia	[45]	359.60	-0.70	9.50	1.33	1.45	2400
4388	B0 III:n	[51]	359.80	-0.60	11.05	0.65	0.94	4250
4389	B1 Ib	[51]	0.19	-0.37	10.23	0.89	1.09	3200
4391	B1 II		359.66	-0.71	10.50	0.88	1.14	2800
4421	B1 III		0.14	-0.82	11.18	0.59	0.85	3700
4424	B2.5 IIIn		359.76	-1.09	11.05	0.58	0.80	2400
4434	B0 Ia	[50]	8.24	3.84	9.25	0.69	0.92	4377

(table con'd)

Table 5: Continued

LSS	Sp. Type	Ref	l(°)	b(°)	V	B-V	E_{B-V}	d(pc)
4443	B0 Ib	[45]	358.29	-2.54	9.85	0.94	1.18	2700
4444	O8 III		359.90	-1.58	10.37	0.67	0.98	4000
4452	B1 III-IV	[51]	1.41	-0.78	9.97	0.51	0.77	2400
4482	B0.5 Ia		7.15	1.83	10.94	1.03	1.24	5900
4502	B1 IVne	[27]	359.53	-3.28	8.26	0.26	0.52	1200
4511	O9 III		6.20	0.40	10.66	0.79	1.10	3500
4513	O6.5 If	[27]	355.36	-6.10	7.32	0.03	0.34	4000
4537	B0.5 Ib		4.85	-0.93	10.85	0.54	0.76	7500
4542	B0.5 Ia		6.79	0.05	9.69	0.83	1.04	4500
4551	O9 Ib		6.49	-0.24	10.45	1.10	1.38	2800
4561	B1 Ib		5.81	-0.80	9.65	0.99	1.19	2100
4565	O6 III	[45]	6.38	-0.50	10.25	1.28	1.60	1800
4567	O9 III	[27]	10.35	1.79	7.48	0.31	0.62	1700
4580	B0 II	[27]	7.34	-0.23	6.74	-0.04	0.25	2100
4597	O9.5 IVn	[27]	6.06	-1.20	7.09	0.00	0.30	1600
4609	B0.5 V		7.67	-0.36	7.26	-0.03	0.25	1000
4614	B1 Ia		3.08	-3.03	10.80	0.61	0.80	10700
4625	BN0 Ia		6.89	-0.93	9.39	0.32	0.55	8100
4626	O5 V	[45]	15.88	4.23	11.10	0.92	1.25	3600
4634	B9 $Ia^{+}{}_{2+}$		357.61	-6.31	11.55	0.46	0.46	52000
4635	O6 Vn((f))	[27]	6.12	-1.48	6.89	0.09	0.42	1600
4653	B0 Ia	[51]	15.12	3.34	7.91	0.55	0.78	2900
4665	O9 IIIn		14.57	2.78	10.85	1.11	1.42	2400
4666	B0.5 Ib	[51]	8.93	-0.44	6.26	0.10	0.32	1700
4781	O9 II	[27]	8.51	-2.32	8.55	0.27	0.58	3300
4800	O7 III		10.70	-1.30	9.49	0.83	1.15	2200
4822	B1 V		11.13	-1.41	11.41	0.54	0.80	2600
4827	B0 II	[51]	12.57	-0.66	8.70	0.50	0.79	2400
4867	O9 V		13.94	-0.33	10.49	0.98	1.29	1500
4872	B2 III		12.06	-1.46	10.13	0.58	0.82	1900
4880	O5 V		18.32	1.87	10.48	0.87	1.20	2900
4882	B3:Ia:	[51]	12.19	-1.56	8.91	0.95	1.07	3100
4896	B0 V(n)		18.26	1.69	10.16	0.63	0.93	1700
4904	B0.5 III	[45]	15.20	-0.10	9.94	0.94	1.22	1400
4910	O7 II		16.98	0.85	9.52	0.84	1.16	2300
4923	O9.5 IIInn		15.70	-0.06	10.45	0.84	1.14	2700
4925	O9 IV		18.22	1.17	10.47	0.89	1.20	2300
4926	O9.5 IV	[51]	17.76	0.88	9.74	1.02	1.32	1200
4930	O6.5 V((f))	[57]	16.02	-0.13	9.40	0.73	1.05	1900
4936	B2.5 $Ibne_1$		16.32	-0.08	11.08	0.71	0.87	6000

(table con'd)

Table 5: Continued

LS	Sp. Type	Ref	l(°)	b(°)	V	B-V	Ref	E_{B-V}	d(pc)
4939	B0.5 III		17.40	0.49	10.54	1.13		1.41	1400
4955	B0.5 Ia		13.13	-1.96	10.12	0.85		1.06	5300
4957	B0 Ib		15.32	-0.78	10.69	0.90		1.14	4250
4967	B0.5 Ia		18.52	0.84	10.01	1.37		1.58	2300
4979	B1 Ia		18.39	0.63	10.00	1.64		1.83	1600
4981	O9.5 V		16.65	-0.35	10.49	0.75		1.05	1900
4991	B1 Ib	[45]	14.99	-1.44	8.02	0.88		1.08	1200
5007	B0.5 Ia(n)		18.98	0.38	8.54	1.37		1.58	1200
5019	O9 Ib		18.68	-0.02	10.63	1.06		1.34	3200
5026	B1 Ia		14.86	-2.23	9.31	0.83		1.02	3900
5046	O7 II		17.99	-0.82	9.27	0.76		1.08	2300
5048	B1 III		17.24	-1.25	9.26	0.50		0.76	1800
5083	O7 IIn		18.63	-1.82	10.00	0.50		0.82	4700
5084	B1 Ia	[51]	16.84	-3.05	7.88	0.84		1.03	2000
5095	O9.5 III		11.80	-6.07	9.60	0.18		0.48	4800
5099	B0.5 Ib		14.62	-4.98	7.09	0.22		0.44	2100
5128	B0.5 Ia		21.62	-4.56	9.83	0.66		0.87	6200
LS									
I +56°087	B0.5 III	[51]	144.28	0.92	6.53	0.33	[51]	0.61	700
I +57°037	B5 Ia	[51]	133.51	-3.57	6.33	0.33	[51]	0.41	2500
I +58°087	B0 III	[51]	136.06	-1.82	8.74	0.49	[51]	0.78	1850
I +58°090	B1 II:	[51]	136.42	-0.95	8.12	0.65	[51]	0.91	1300
I +60°158	B3 Ia	[51]	127.38	-2.28	7.87	0.46	[18]	0.58	4000
I +60°245	B0 Ib	[47]	135.00	0.00	8.850	0.640		0.880	2700
I +60°257	B5 Ib	[47]	136.00	1.00	10.43	0.75		0.85	4200
I +60°291	O7 V(n)	[26]	138.03	1.50	7.82	0.38	[51]	0.70	1400
I +61°121	O8 Ib(f)	[26]	117.44	-0.14	8.20	0.27	[59]	0.56	3300
I +61°234	B0.5 Ib	[67]	129.48	-0.66	9.77	0.58	[67]	0.80	4300
I +61°286	O4 If+	[28]	134.77	0.86	8.10	0.70	[51]	1.03	2100
I +61°293	O5 V((f))	[28]	134.77	1.01	8.43	0.42	[51]	0.75	2200
I +62°023	B3 Ia	[51]	115.79	1.24	8.65	1.09	[51]	1.21	2300
I +62°128	B0.7 Ia	[26]	120.84	0.14	4.16	0.14	[59]	0.33	1000
I +62°150	B0 III	[65]	124.95	-0.01	10.42	0.77	[51]	1.06	2700
I +62°157	B5 Ia	[51]	126.71	0.16	8.74	0.91	[51]	0.99	3300
I +62°220	B0.5 Ib	[47]	134.00	2.00	10.19	0.69		0.91	4400
I +62°224	B0 IIInn	[47]	135.00	2.00	9.69	0.55		0.84	2800
I +63°031	B3 Ia	[60]	117.63	1.26	6.24	0.33	[51]	0.45	2300
I +63°057	B0 IIIe1	[47]	119.00	1.00	10.27	0.52		0.81	3900
I +63°116	B1.5 Ia	[26]	123.71	0.85	7.71	0.62	[51]	0.80	2600
I +64°017	B0.5 Ib	[47]	118.00	2.00	9.64	0.56		0.78	4200

(table con'd)

Table 5: Continued

LS	Sp. Type	Ref	l(°)	b(°)	V	B-V	Ref	E_{B-V}	d(pc)
I +66°007	B1 Ib	[47]	121.00	4.00	10.20	0.88		1.08	3200
II +11°009	B0 Ib:n	[68]	49.39	-5.29	9.36	0.14	[69]	0.38	7100
II +12°003	O9 III		45.00	2.00	10.72	1.00		1.31	2700
II +12°009	O9 III	[47]	49.00	-3.00	11.28	0.19		0.50	11400
II +14°008	B1 Vne_{2+}		48.00	1.00	10.68	0.68		0.94	1600
II +15°001	B3 $IIIne_1$		45.00	9.00	11.27	0.41		0.61	3100
II +16°008	B1 III		52.00	0.00	10.63	1.09		1.35	1400
II +16°012	O9.5 Ib	[47]	53.00	-2.00	10.55	0.63		0.89	5900
II +17°010	B1 III		54.00	-1.00	11.22	0.73		0.99	3100
II +20°013	O9.5 IV		57.00	-1.00	10.90	0.99		1.29	2200
II +23°048	B1 Ia	[51]	60.41	-0.29	7.85	0.79	[51]	0.98	2100
II +27°007	B0.5 Ib	[47]	62.00	2.00	10.27	0.39		0.61	7100
II +33°012	B1.5 III	[47]	70.00	2.00	11.27	0.46		0.71	4300
II +33°034	B2 IIe	[47]	74.00	-3.00	10.01	0.87		1.10	2000
II +34°026	B1.5 Ibe	[47],[34]	76.00	-5.00	11.07	0.17		0.36	14100
II +36°037	B2 III	[47]	74.00	1.00	11.30	0.33		0.57	4700
II +39°053	O7 V:		78.00	0.00	10.34	1.01		1.33	2000
II +40°008	O5 V	[47]	77.00	3.00	9.49	0.97		1.30	1600
III +41°001	B0 III	[75]	77.43	6.17	7.81	0.02	[18]	0.31	2400
III +41°014	O9 V	[76]	79.01	3.63	10.97	0.60	[70]	0.91	3200
III +41°029	O7 III((f))	[71]	80.22	1.02	10.22	1.18	[63]	1.50	1800
III +41°039	O9.5 Ia	[51]	80.47	0.85	9.89	1.53	[51]	1.78	1600
III +44°017	O9.5 Ia	[51]	82.36	2.96	7.08	0.87	[51]	1.12	1200
III +44°041	O9.5 Ib	[51]	87.29	-2.66	7.80	0.22	[51]	0.48	3000
III +45°054	B3 Ib	[47]	87.00	-1.00	11.52	0.38		0.52	11800
III +46°001	O9.5 Iab	[73]	80.99	10.09	5.61	-0.05	[73]	0.20	1900
III +46°002	B1.5 Vne	[26]	81.86	7.93	8.36	0.24	[18]	0.49	800
III +46°012	O4 III	[47]	84.00	3.00	10.26	0.97		1.30	3300
III +46°019	B0.5 III	[47]	85.00	2.00	11.38	0.61		0.89	4500
III +46°026	B0.5 Ibe	[47]	85.00	1.00	10.61	0.61		0.80	6500
III +46°050	O9 III	[47]	88.00	-1.00	10.70	0.69		1.00	4200
III +47°018	B0 II-III	[51]	87.61	2.11	9.79	0.77	[51]	1.06	2600
III +47°020	B8 Iae	[51]	87.51	1.42	5.66	0.47	[51]	0.49	1700
III +52°030	O9 Ib	[51]	99.85	-3.13	7.54	0.05	[51]	0.33	3400
III +54°010	B1: V:nne		100.39	-0.25	10.29	0.46	[51]	0.72	1700
III +55°008	B0 IV	[47]	95.00	5.00	10.36	0.64		0.93	2600
III +55°019	B0.5 III	[47]	100.00	1.00	10.64	0.63		0.91	3100
III +55°020	O9 III::	[47]	100.00	0.00	11.11	0.73		1.04	5200
III +55°026	O9 V	[47]	101.00	0.00	11.42	0.40		0.71	5400

(table con'd)

Table 5: Continued

LS	Sp. Type	Ref	l(°)	b(°)	V	B-V	Ref	E_{B-V}	d(pc)
III +57°017	B0 V:pe	[51]	99.80	3.62	6.91	0.21	[51]	0.51	700
III +57°024	B5 Ia:	[47]	102.00	1.00	10.60	0.93		1.01	8200
III +57°027	B2 Iae	[47]	102.00	1.00	9.66	1.34		1.50	2600
III +57°112	B0 III	[47]	108.00	-1.00	10.55	0.80		1.09	2700
III +58°053	B1 Ib	[47]	107.00	0.00	10.31	1.13		1.33	2300
III +58°064	B1 Ia		108.03	-0.35	7.20	0.60	[51]	0.79	2100
III +58°070	O9.5 V	[74]	108.81	-1.01	11.30	0.46	[74]	0.76	4200
III +59°011	B0 V	[51]	101.60	4.67	7.31	0.33	[51]	0.63	700
III +59°019	B0.5 III	[47]	103.00	3.00	11.04	0.56		0.84	4200
III +59°029	B0.5 III	[47]	107.00	0.00	11.14	0.68		0.96	3700
III +59°051	B0 Ia	[51]	110.81	-1.18	8.91	1.02	[51]	1.25	2300
III +59°056	O9 IIIe3	[47]	111.00	0.00	9.52	0.59		0.90	3000
III +59°058	O9.5 III	[47]	111.00	0.00	10.91	0.47		0.77	5700
III +60°046	B1.5 II	[51]	110.93	0.07	9.68	0.84	[72]	1.08	1800
III +60°068	O6.5 III	[64]	112.23	0.22	8.67	0.41	[51]	0.73	2900
III +61°002	B2 Ib	[26]	102.27	7.25	4.72	0.30	[22]	0.48	600
III +61°021	B0 III:p	[51]	111.95	1.27	9.70	0.79	[51]	1.08	1850
III +61°023	B0.5 Ib:		112.06	1.02	10.23	1.00	[51]	1.22	2850
III +61°028	B1 III	[47]	112.00	0.00	11.13	0.63		0.89	3400
III +62°003	B0.5 V	[55]	103.11	6.82	7.50	0.25	[78]	0.53	800
III +62°007	O9.5 Ib	[51]	104.87	5.39	5.10	0.09	[51]	0.35	1100
III +63°026	B0 II	[51]	112.89	3.10	8.46	0.71	[51]	1.00	1550
III +63°028	B0.5 Ib	[47]	113.00	2.00	11.04	0.63		0.85	7100
III +63°029	O7 Ib(f)	[47]	114.00	2.00	10.91	0.90		1.21	5200
III +64°003	B0.5 Ibe	[51]	108.50	6.39	5.46	0.37	[51]	0.59	800
III +64°011	B0.5 Ia	[66]	110.93	4.31	9.08	0.85	[51]	1.06	3300
IV +03°011	B3 Ia	[51]	37.81	-1.95	7.41	0.50	[51]	0.62	3100
IV +05°005	O9 II	[47]	37.00	5.00	10.97	0.56		0.87	6600
IV +08°005	B1 Ia	[68]	45.04	-4.82	9.86	0.25	[68]	0.44	11800
IV +10°002	B0.5 Ib	[47]	41.00	4.00	10.64	0.26		0.48	10300
IV +11°005	B1 Ia:	[51]	44.21	2.66	10.57	1.04	[51]	1.23	5100
IV -01°004	B8 Ia:	[68]	30.71	1.48	9.22	1.50	[68]	1.52	1950
IV -02°005	B0.5 III	[75]	23.64	12.90	7.78	0.22	[77]	0.50	1500
IV -04°015	O6 Ib(f)		27.00	0.00	10.37	0.90		1.22	4400
IV -04°021	B0.5 Ia	[51]	28.16	-0.77	8.23	0.80	[51]	1.01	2400
IV -04°025	O9.5 Ia		28.00	-1.00	10.51	0.95		1.20	5100
IV -06°039	B0.5 Iab	[68]	26.85	-2.31	8.92	0.36	[68]	0.57	5000
IV -07°016	B1: V:npe	[51]	25.82	-1.71	7.80	0.22	[51]	0.48	800
IV -07°029	B1 Ia	[68]	27.22	-4.99	9.55	0.33	[68]	0.52	9100

(table con'd)

Table 5: Continued

LS	Sp. Type	Ref	l(°)	b(°)	V	B-V	Ref	E_{B-V}	d(pc)
IV -08°008	B0.5 III		22.88	0.66	10.52	1.09	[18]	1.37	1500
IV -08°009	O9: V:p	[73]	23.79	0.06	9.44	0.91	[73]	1.22	1000
IV -08°011	B2 Ib(n)		23.00	0.00	10.20	0.86		1.04	3600
IV -08°019	B0.5 V	[51]	23.96	-1.62	7.62	0.54	[51]	0.82	500
IV -08°028	O9.5 III		27.00	-6.00	11.46	0.13		0.43	12200
IV -10°002	O6.5 III(f)	[28]	12.97	13.31	7.78	0.17	[77]	0.49	2800
IV -11°002	B0 V	[77]	13.42	12.24	10.27	0.21	[18]	0.51	3400
IV -11°002	B0 V	[47]	13.00	12.00	10.27	0.21		0.51	3400
IV -11°021	B0.5 Ia	[51]	20.02	0.24	8.38	1.06	[51]	1.27	1750
IV -12°006	B1 Ib	[47]	17.00	2.00	8.62	0.95		1.15	1400
IV -15°039	B2 Ib	[79]	15.36	0.39	9.46	0.31	[18]	0.49	5200
IV -15°039	B0.5 III	[47]	15.00	0.00	9.46	0.31		0.59	2900
V +20°004	O8: V:nn	[51]	187.89	-2.51	9.29	0.24	[51]	0.56	3000
V +20°011	B2 Ia	[21]	189.69	-0.86	4.63	0.27	[80]	0.43	1100
V +23°056	B0 II		188.49	3.87	6.92	0.29	[51]	0.58	1400
V +25°011	B1 Ib	[51]	183.97	0.84	4.81	-0.06	[51]	0.14	1100
V +25°029	B1 Vne	[81]	187.26	5.74	8.44	0.07	[18]	0.33	1300
V +28°024	B2 Ib	[51]	182.26	3.87	7.46	0.32	[51]	0.50	2050
V +33°033	B0.5 V	[51]	173.73	-0.51	7.44	0.12	[51]	0.40	900
V +34°023	B0.5 IV	[51]	173.24	-0.20	8.04	0.32	[51]	0.60	1200
V +37°004	B1 Ib	[47]	167.00	-2.00	11.45	0.51		0.71	9900
V +37°010	O7 II	[28]	170.04	0.27	6.79	0.02	[73]	0.34	2200
V +45°017	B0.5 III	[47]	160.00	1.00	10.60	0.64		0.92	3000
V +47°022	B0 V	[74]	159.36	2.59	12.10	0.52	[74]	0.82	5000
V +51°019	B0 II	[51]	152.58	1.95	9.63	0.73	[51]	1.02	2600
V +53°005	B1 Ib	[47]	142.00	-3.00	10.22	0.66		0.86	4500
V +53°021	B0 III	[47]	151.00	2.00	10.93	0.64		0.93	4100
V +53°024	B0 III	[75]	151.91	3.95	5.77	0.18	[18]	0.47	700
V +56°003	B2 Ib	[51]	134.38	-3.93	7.37	0.23	[51]	0.41	2200
VI +00°007	B2 Ib	[51]	210.24	-3.72	9.12	0.71	[82]	0.89	2500
VI +02°010	O7 III((f))	[26]	208.73	-2.63	7.95	0.33	[51]	0.65	2300
VI +02°011	B2 III		208.93	-2.66	11.26	0.69	[18]	0.93	2700
VI +04°036	O7 V	[47]	208.00	1.00	10.69	0.33		0.65	5800
VI +06°012	B2 Vnne2		207.18	2.43	10.80	0.28	[18]	0.52	2100
VI +10°011	B0.5: V		202.05	1.32	7.77	0.41	[18]	0.69	700
VI -01°005	B8 Ia:		212.86	-3.41	10.14	0.84	[18]	0.86	7900
VI -01°015	B0.5 III		215.13	0.44	9.92	0.46	[51]	0.74	2900

classes. There is general agreement between this plot and earlier work, by Georgelin and Georgelin [11] and Walborn [12] in the region common to the plots. Walborn's study covers a distance of up to 5 kpc from the sun. The following features can be noted:

a) We find O and B type stars up to 6 kpc from the Sun in the Puppis window (at $l = 245°$).

b)The Carina feature at $l \approx 288°$ continues out to a larger distance than ever reported. The Carina arm which points away from the Sun, is shown clearly separated from the Puppis region. This agrees well with the space distribution of O stars in the solar neighbourhood as derived by Walborn [12]. The absence of stars in the longitude range $\approx$268 to $\approx$280 could of course be due to the presence of obscuring material in this region. Fitzgerald [48] and Neckel and Klare [49] report dust clouds extending about a kpc with extinction of more than 1 magnitude per kpc in this region. However, even if the extinction in this direction were 3 magnitudes, O supergiants of $M_V = -6.8$ at a distance of 14 kpc should have been visible in this survey that was complete to the 12th B magnitude. This would imply either that there are dust clouds beyond the region of the study by Neckel and Klare, or that there are indeed no young stars in this region.

c) There seems to be a feature extending to a considerable distance in the direction of $l \approx 308°$. Georgelin et al [83] studied this region using Hα and radio data and found a number of H II regions lying at varying distances between 2 and 11 kpc in this longitude interval. They suggest that these H II regions belong to the Scutum-Crux arm.

d) In Fig. 4 the spiral arms as derived by Georgelin and Georgelin [11] are shown plotted on the distribution in Fig. 3. In Fig. 5 the spiral arms as derived by Walborn [12] as a possible structural interpretation of the distribution of O stars are shown plotted on the distribution of Fig. 3. We note that we do not see the the clear gap between the local feature and the inner edge of the Perseus arm as seen in Walborn's plot of O stars. The fact that Fig. 3 also includes stars of later spectral types, combined with the distance errors, could have smeared out the distribution.

The errors in the distances come from several sources:

1) Variations and errors in calibrations: There are differences in absolute magnitude of 0.2 to 0.3 magnitudes between different sources, leading to errors of the order of 10%-15%. Also, as mentioned in chapter 3, stars of a given spectral type really do have a range of luminosity, so that there is an intrinsic scatter in the calibrations. Uncertainty in spectral types must contribute significantly to errors in calibration.

2) Errors due to uncertainty in spectral types: For a given calibration, this is usually the largest source of error in the determination of distance. In the worst possible case, an error of one luminosity class between B1 III and B1 V, where the change in absolute magnitude with luminosity class is the largest, can lead to an error of more than 50% in the distance.

3) Errors from using calibrations of normal stars on peculiar stars that are not detected as peculiar spectroscopically. It is possible to have stars of different luminosities that have identical spectra, provided the ratio of the mass to the square of the radius is the same for each star. For a given chemical composition, the spectrum is determined by the effective temperature T_{eff} and

surface gravity g. $\sigma T_{\mathrm{eff}}^4 = L/4\pi R^2$ and $g = GM/R^2$. A star that has 1/2 the radius but 1/4 the mass will have 1/4 the luminosity, and will look identical spectroscopically. An example of this is LSS 4634; the spectrum of this star is that of a B9 supergiant. If this were a normal star of absolute magnitude –8.5 , it would be at a distance of more than 50 kpc from the Sun. Its infrared colors however are like those of a planetary nebula [33] and it appears to be a low-mass star that is evolving off the asymptotic giant branch. But this would only occur in rare cases.

4) Errors from non-uniformity of A_V/E_{B-V}. If there are local variations in the absorption to extinction ratio, the distance would be affected.

Distribution perpendicular to the plane

It is known that the Carina arm bends in both l and b; from 21 cm observations [85], it has been shown that the Galactic disk has a warp about the $l = 10°$ direction, bending to negative latitudes in the direction of $l = 270°$ and positive latitudes in the direction $l = 90°$. Noticing that most of the OB^+ stars in the southern Milky Way seem to lie below the $b = 0°$ plane, plots of z, the distance from the plane versus distance were made in various longitude zones, as shown in Fig. 6. The choice of the zones was made rather arbitrarily, guided by the distribution shown in Fig. 2. We do see a clear trend toward negative z values, which gets less pronounced as $l = 10°$ is approached. The warp in the stellar component appears to start between 4 and 6 kpc from the sun. In the longitude range 0° to 20°, there is no preference for either direction and the stars are equally distributed above and below the plane, consistent with the radio data. It is of course possible that no stars are seen above (or below) the plane because of concentration of obscuring material at these longitudes.

However, from his study of the distribution of reddening material within 3 kpc from the sun, FitzGerald [48] concluded that the extinction is greatest at or near z=0 for most directions in the Galactic plane. The only exception he found was for l between 190° and 220° degrees, where the extinction was found to be a maximum (of about .6 magnitudes/kpc) at $z = -200$pc; but this region is not shown in Fig. 6 because, as Fig. 2 shows, there are few OB^+ stars between these longitudes. Also, for l between 220° and 250°, he found a color excess of about .2 magnitudes/kpc from $z = -300$ to $+300$ pc; i.e., the extinction is equal above and below the plane. Therefore it seems unlikely that the distribution shown in Fig. 6 is due to the obscuring material.

4.2 Distribution of Dust

From the data presented in Table 5, the distribution of dust near the Galactic equator can be deduced. Figs. 7, 8, and 9 show the distribution of color excess, projected on the Galactic plane in layers of different thicknesses. The size of the circles indicates the value of the color excess; the smallest indicates a color excess of less than .23 magnitudes. Each larger circle represents a color excess of .22 magnitudes greater than the previous one. An attempt was made to map the extinction as a function of z in specific longitude intervals; but because of the small number of stars, it did not prove very useful.

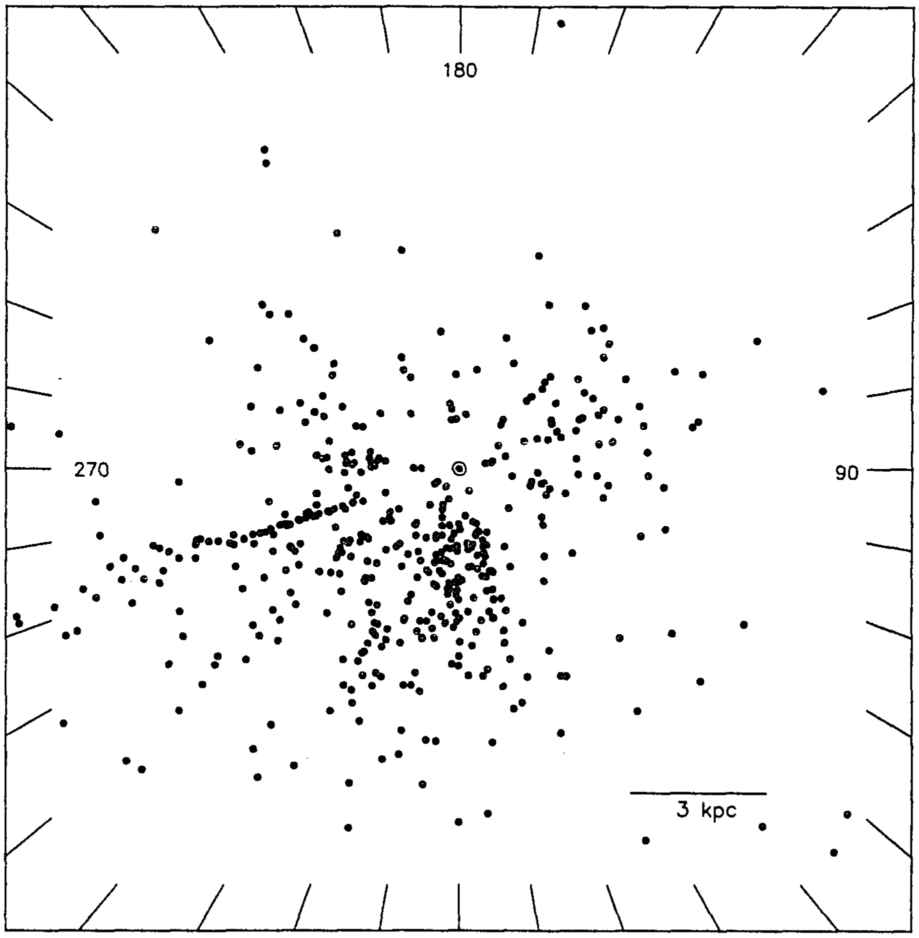

Figure 2. The OB$^+$ stars projected onto the Galactic plane. The sun is at the center of the plot.

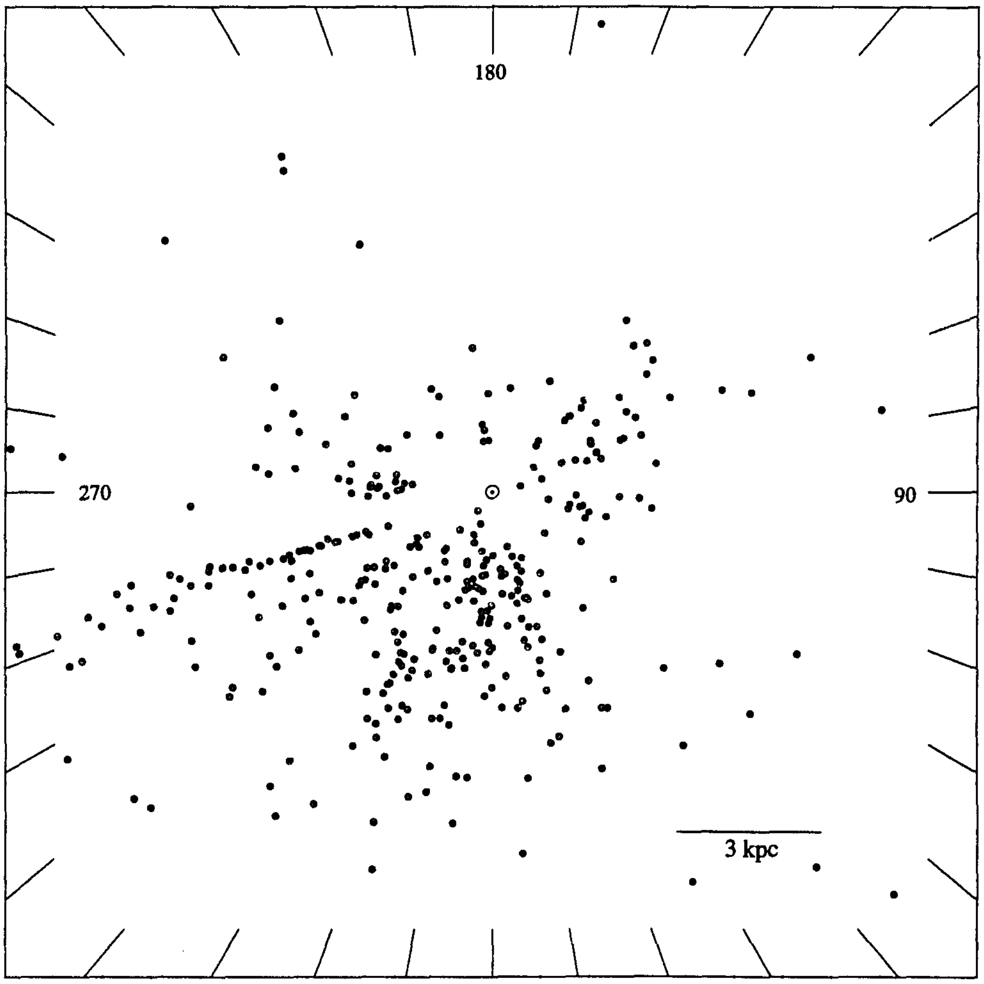

Figure 3. The O3-O8 stars of all luminosity classes, and supergiants of later spectral types, projected on to the Galactic plane. The sun is at the center of the plot.

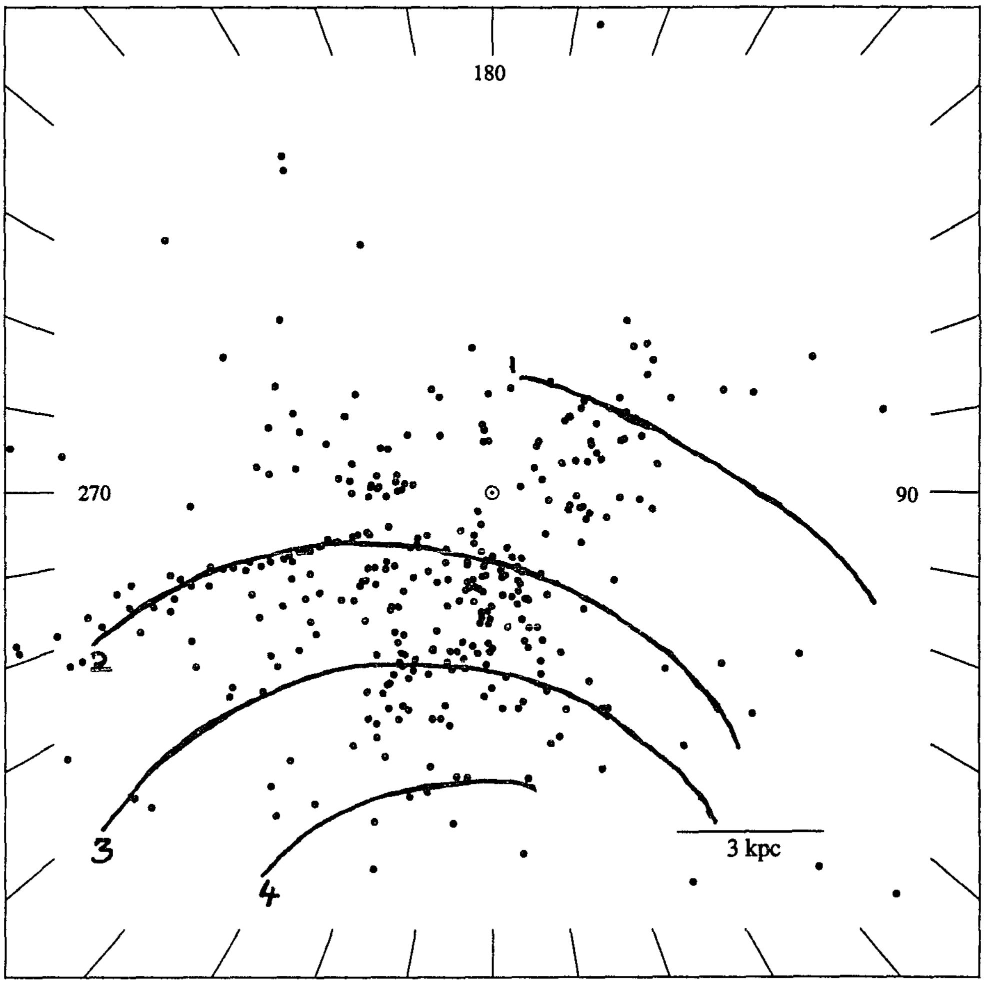

Figure 4. The distribution shown in Fig.3, with the spiral arms as derived by Georgelin and Georgelin [11]. 1: Perseus arm; 2: Carina-Saggitarius arm; 3: Scutum-Crux arm; 4: Norma arm.

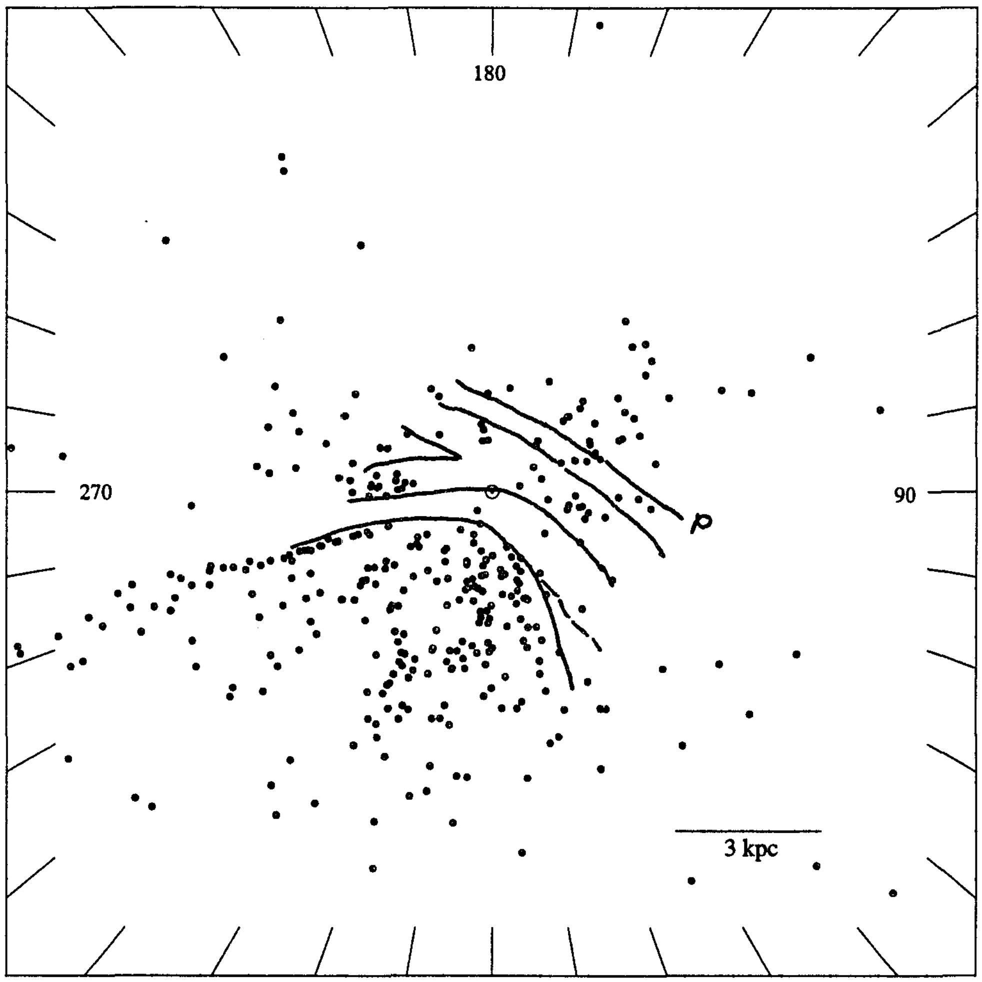

Figure 5. The distribution shown in Fig.3, with the spiral arms as derived by Walborn [12]. 'P' marks the inner edge of the Perseus arm.

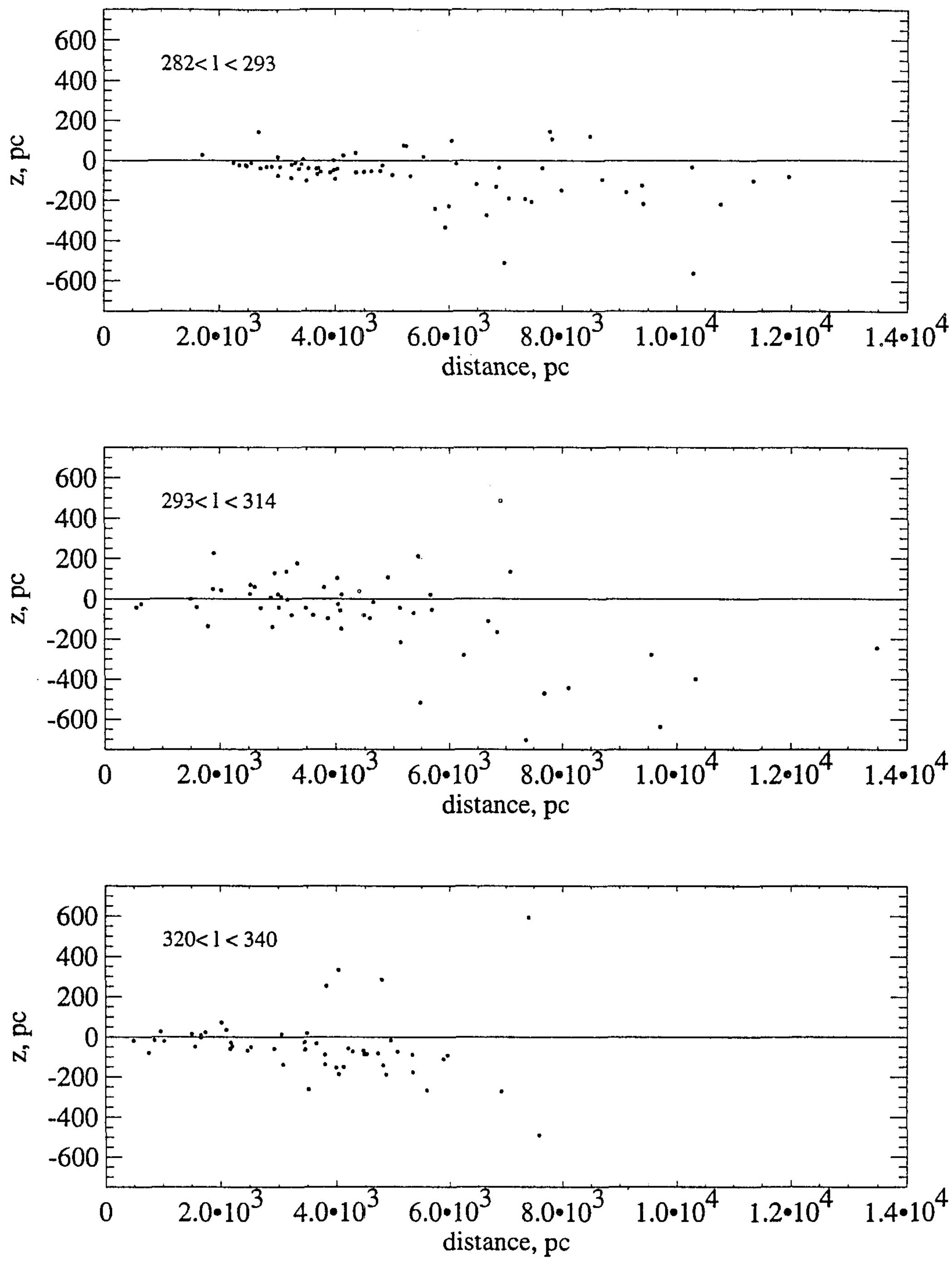

Figure 6. The distribution of stars perpendicular to the plane for various longitude sections.

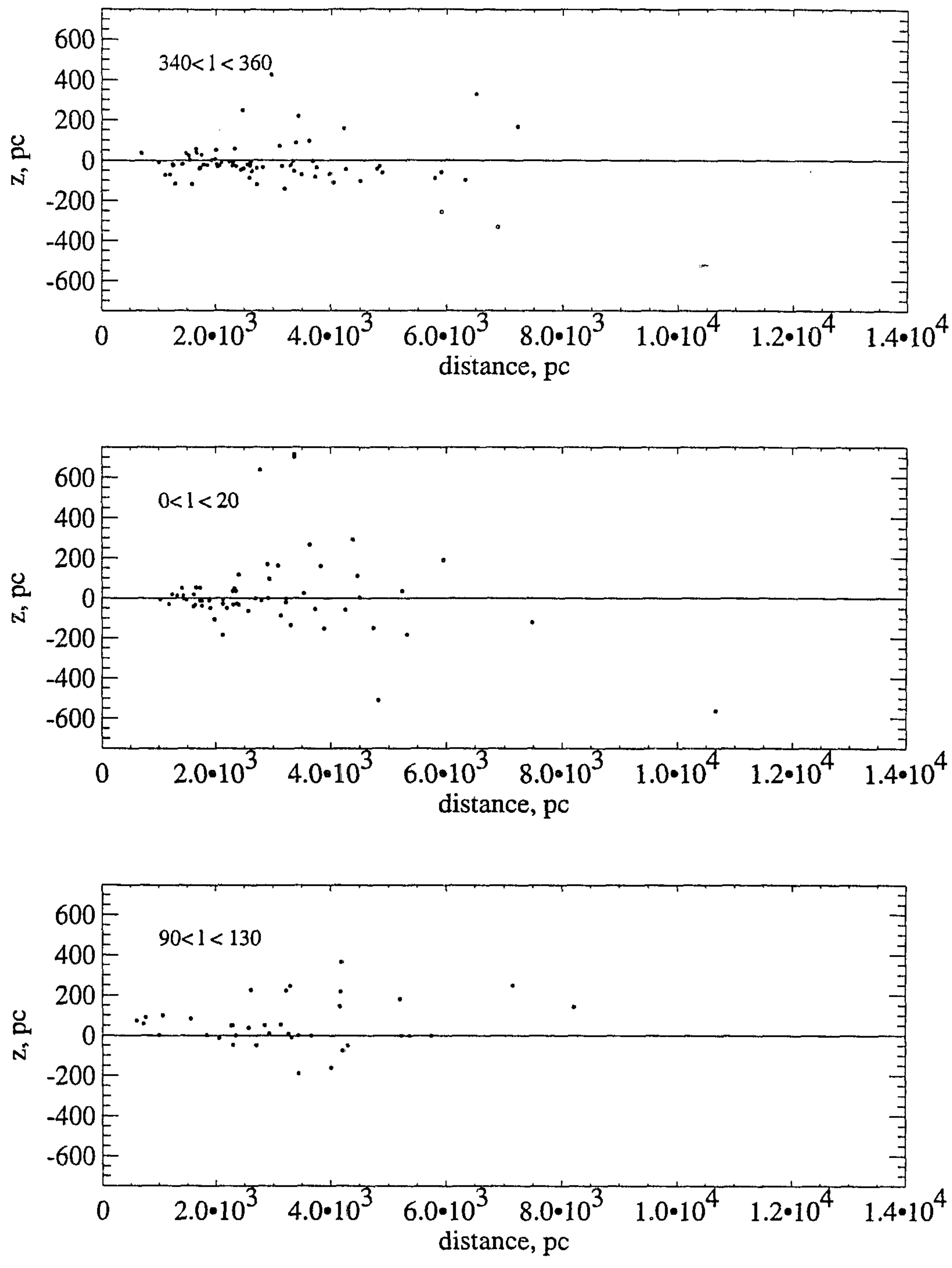

Figure 6: Continued

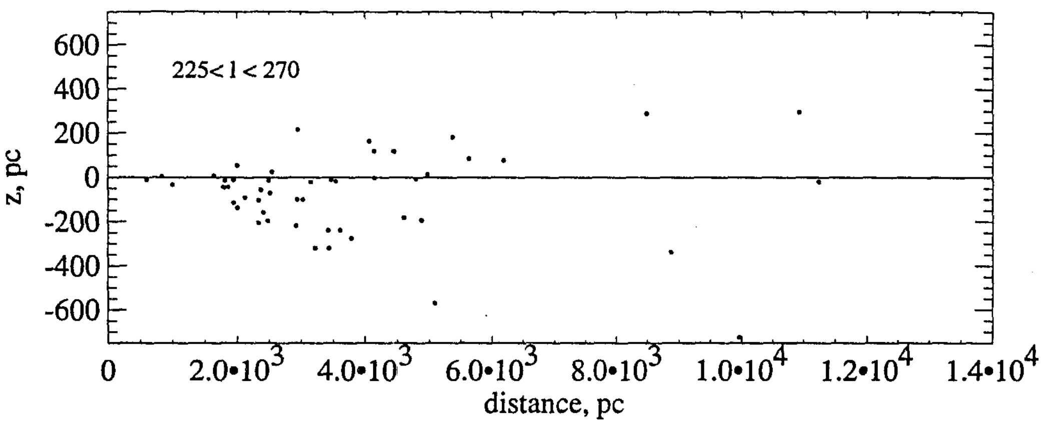

Figure 6: Continued

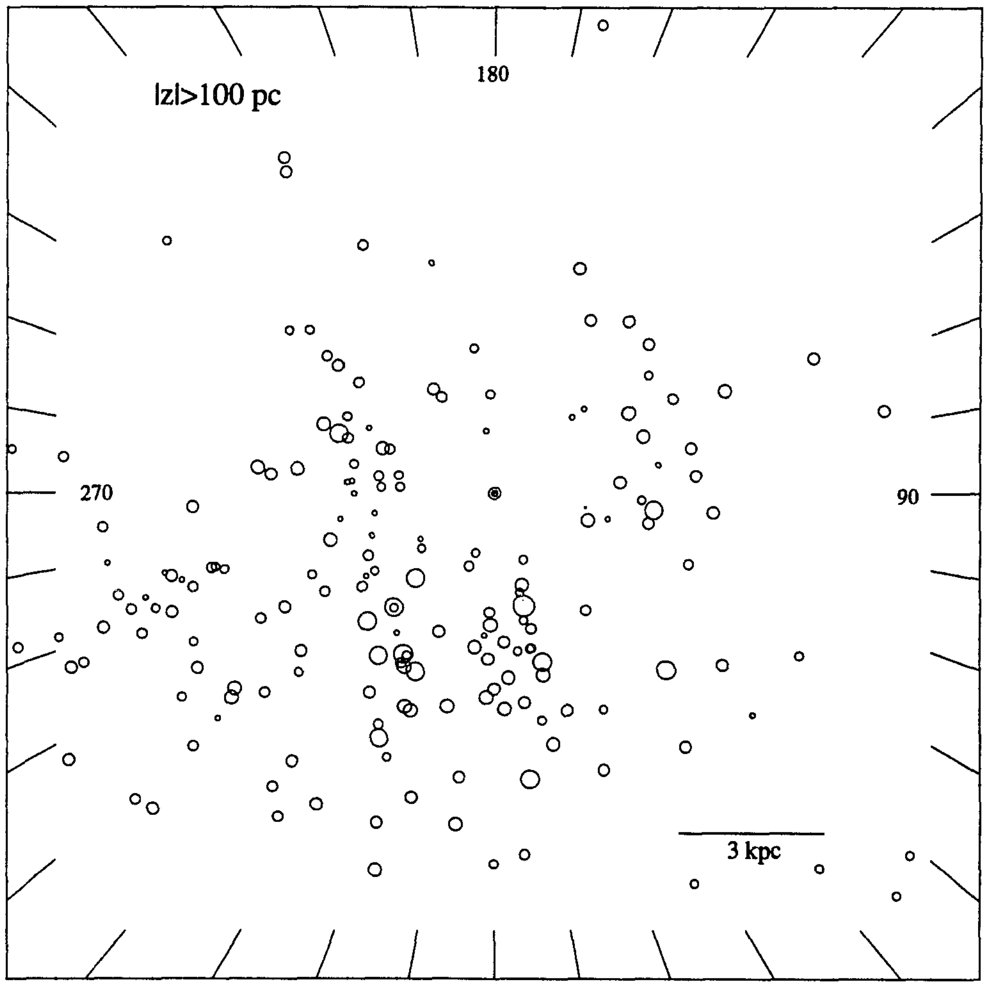

Figure 7. Color excesses for stars shown in Fig. 2 that are beyond ± 100 pc from the b=0° plane.

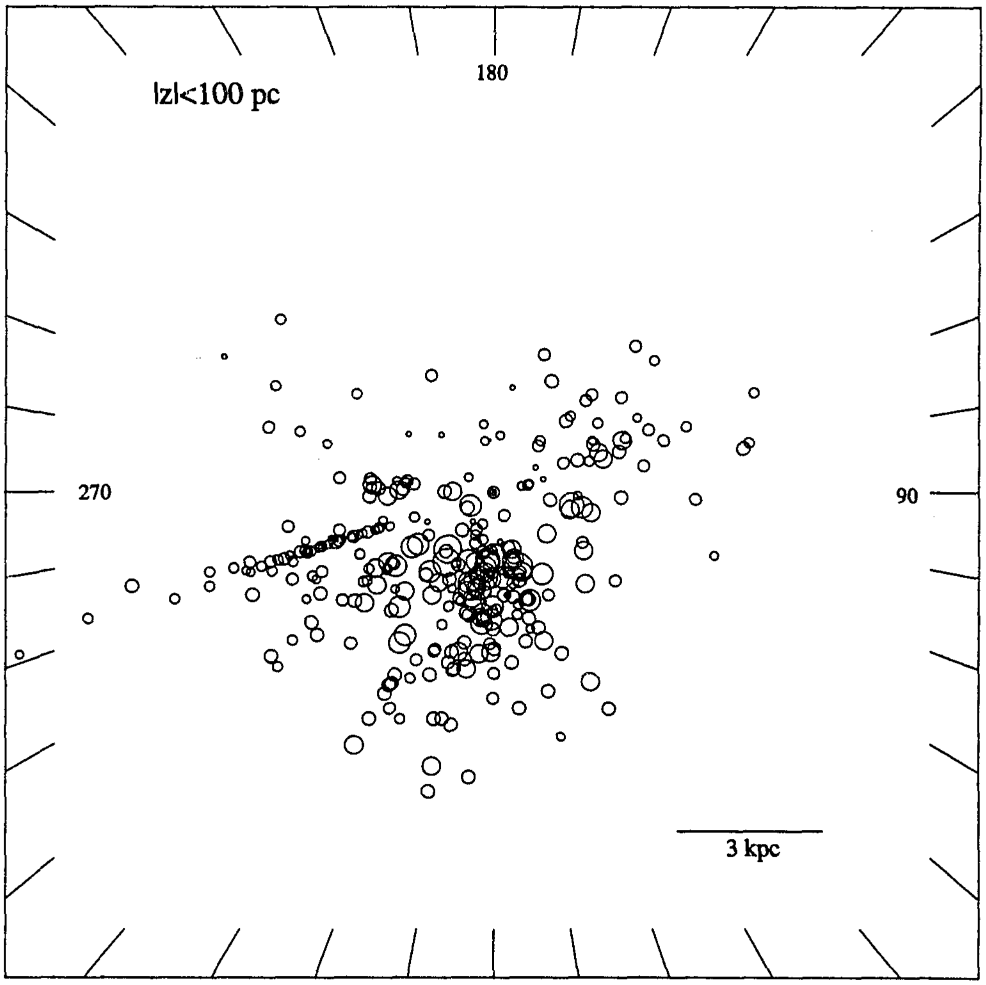

Figure 8. Color excesses for stars shown in Fig. 2 that are within ± 100 pc from the b=0° plane.

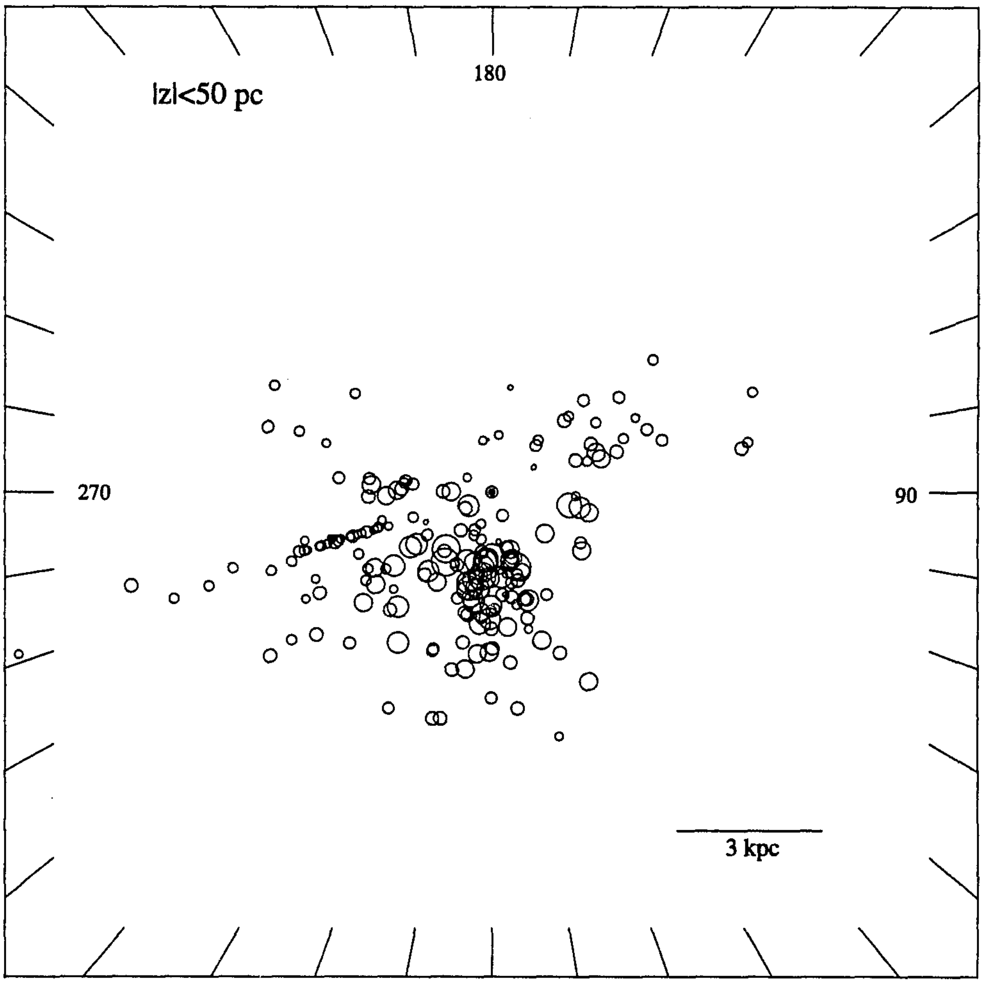

Figure 9. Color excesses for stars shown in Fig. 2 that are within ± 50 pc from the b=0° plane.

CHAPTER 5

SUMMARY

We have computed the distances to a complete set of OB^+ stars down to the 12th B magnitude and mapped their space distribution. Since the limiting magnitude of the survey from which the program stars were taken was as faint as 12, this map extends to larger distances than any previous study of Galactic structure at optical wavelengths. There is agreement between this study and earlier work in the region where they overlap.

The bend in the Galactic disk toward negative latitudes in the south and positive latitudes in the north is consistent with radio study. However, while this cannot be ruled out as being due to dust in the regions where no stars are seen, it seems unlikely. Comparison with maps of interstellar dust up to 3 kpc shows no systematic preference of dust in the positive latitudes in the south and negative latitudes in the north to explain the absence of stars in these regions. Besides, as was pointed out in Chapter 4, the intrinsically bright stars that comprise our sample should be easily seen out to several kpc even if the extinction is a few magnitudes.

The map of color excesses clearly shows that the dust is very patchy. There is no clear increase of color excess with distance in the disk; one reason for this is of course the large errors in the distances.

We are limited in the mapping of dust by the fact that we can only get color excesses in the direction of the stars. Our resolution is therefore not good enough to show the large dust clouds on the inner edge of the spiral arms as seen in the photographs of other galaxies. Also, the number of OB^+ stars is too small to get contour maps of extinction, as has been done in the solar neighborhood.

During spectral classification, several objects that had peculiar spectra were found. Also, one object which had a normal spectrum but turned out to be a very interesting object was found; its distance, calculated using calibrations of normal stars would have put it well outside our Galaxy; a search through the SIMBAD data base revealed that this star had infrared colors like that of a planetary nebula. This object, which lies at $b = -6.3°$, has the spectrum of a supergiant, and was found to be a variable, has all the properties of post-asymptotic giant branch objects described by Parthasarathy [34].

Other peculiar stars that were picked out are ones with anomalous nitrogen line strengths, emission line stars that could be H-poor, and binary stars. Several He stars, and a complete sample of sdO stars have been studied and discussed by Drilling [12, 13].

REFERENCES

[1] Stephenson, C. B. and Sanduleak, J., Luminous Stars in the Southern Milky Way, Publ. of the Warner and Swasey Observatory, vol.1. #1 (1971)

[2] Hardorp, J., Rohlfs, K. Slettebak, A. and Stock, J. Luminous Stars in the Northern Milky Way (Hamburg–Bergedorf: Hamburger–Sternwarte and Warner and Swasey Observatory) (1959)

[3] Stock, J., Nassau, J. J., and Stephenson, C. B. Luminous Stars in the Northern Milky Way (Hamburg–Bergedorf: Hamburger–Sternwarte and Warner and Swasey Observatory) (1960)

[4] Hardorp, J., Theile, I. and Voigt, H. H.Luminous Stars in the Northern Milky Way (Hamburg–Bergedorf: Hamburger–Sternwarte and Warner and Swasey Observatory) (1964)

[5] Nassau, J. J., and Stephenson, C.B. Luminous Stars in the Northern Milky Way (Hamburg–Bergedorf: Hamburger–Sternwarte and Warner and Swasey Observatory) (1963)

[6] Hardorp, J., Theile, I. and Voigt, H. H. Luminous Stars in the Northern Milky Way (Hamburg–Bergedorf: Hamburger–Sternwarte and Warner and Swasey Observatory)(1965)

[7] Nassau, J. J., and Stephenson, C. B. and MacDonnell, D. J. Luminous Stars in the Northern Milky Way (Hamburg–Bergedorf: Hamburger–Sternwarte and Warner and Swasey Observatory) (1965)

[8] Whittet, D. C. B., van Breda, I. G. and Glass, I. S. MNRAS 177 625 (1976)

[9] Verschuur, G. L. ARAA 13 257 (1975)

[10] Burton, W. B. in Galactic and Extragalactic Radio Astronomy, Springer-Verlag, Verschuur, G. L. and Kellerman, K. I. Eds, (1988)

[11] Georgelin, Y. M., and Georgelin, Y. P. AA 49 57 (1976)

[12] Walborn, N. R. AJ 78 1067 (1973)

[13] Reed, B. C. PASP 105 1469 (1993)

[14] Morgan, W. W., Sharpless, S. and Osterbrock, D. E. AJ 57 3 (1952)

[15] Reed, B.C. AAS 77 447 (1989)

[16] Kimeswenger, S. and Weinberger, R. AA 209 51 (1989)

[17] Drilling, J. S. ApJ Suppl 76 1033 (1991)

[18] Drilling, J. S. AJ 80 128 (1975)

[19] Walborn, N. R. ApJ 164 L67 (1971)

[20] Cannon, A. Annals of the Astronomical Observatory of Harvard College 56 65 (1912)

[21] Morgan, W. W., Keenan, P. C. and Kellman, E. An Atlas of Stellar Spectra, Chicago University Press, Chicago, (1943)

[22] Johnson, H. L. and Morgan, W. W., ApJ 117 313 (1953)

[23] Morgan, W. W. and Keenan, P.C. ARAA 11 29 (1973)

[24] Morgan, W. W., Abt, H. A. and Tapscott, J.W., Revised MK Spectral Atlas for Stars Earlier than the Sun (Yerkes Observatory) (1978)

[25] Walborn, N. R. ApJ 254 L15 (1982)

[26] Walborn, N. R. ApJS 23 257 (1971b)

[27] Garrison, R.F., Hiltner, W. A. and Schild, R. E. ApJ 35 111 (1977)

[28] Walborn, N.R. AJ 77 312 (1972)

[29] Hiltner, W. A., Garrison, R.F. and Schild, R. E. ApJ 157 313 (1969)

[30] Yamashita, Y., Nariai, K. and Norimoto, Y. An Atlas of Representative Stellar Spectra (University of Tokyo Press, Tokyo) (1978)

[31] Schönberner, D. et al, AA 197 209 (1988)

[32] Walborn, N. R. ApJ 205 419 (1976)

[33] Preite-Martinez, A. AAS 76 317 (1988)

[34] Parthasarathy, M. ApJ 414 L109 (1993)

[35] Kilkenny, D. et al IBVS 3659 (1991)

[36] Landolt, A. U. and Drilling, J. D. AJ 91 1372 (1986)

[37] Drilling, J. S. and Hill, P. W. in IAU Colloquium No. 87, Hydrogen Deficient Stars and Related Objects, K. Hunger, D. Schönberner and K. Rao, eds., Reidel, Dordrecht, 499 (1986)

[38] Drilling, J. S. in IAU Colloquium No. 87, Hydrogen Deficient Stars and Related Objects, K. Hunger, D. Schönberner and K. Rao, eds., Reidel, Dordrecht, 9 (1986)

[39] Drilling, J. S. in The Atmospheres of Early Type Stars, Heber U., Jeffery, C. S. eds, Springer-Verlag, Berlin, 257 (1991)

[40] Drilling, J. S. ApJ 294 L107 (1985)

[41] Drilling, J. S. AA 71 214 (1979)

[42] Drilling, J. S. in IAU Colloquium NO. 95, The Second Conference on Faint Blue Stars, A. G. Davis Philip, D. S. Hayes and J. W. Liebert, eds., L. Davis Press, Schenectady, NY, 489 (1987)

[43] Drilling, J. S. AA 71 214 (1979)

[44] Schmidt-Kaler, Th. in Landolt Bornstein, New Series, Group VI vol. 2 (1982)

[45] Drilling, J. S. and Perry, C. L. AAS 45, 439 (1981)

[46] Humphreys, R. M. AAS 9 85 (1973)

[47] Drilling, J. S. (unpublished)

[48] FitzGerald, M. P. AJ 73 983 (1968)

[49] Neckel, Th. and Klare, G. AAS 42 251 (1980)

[50] Sandage, A. and Wallerstein, G. ApJ 131 598 (1960)

[51] Hiltner, W.A. ApJS 2 389 (1956)

[52] Bassino, L. P. et al MNRAS 201 885 (1982)

[53] Mathys, G. Astronomy and Astrophysics 81 237 (1989)

[54] Smith, M. A. ApJ 203 603 (1976)

[55] Walker, G.A.H. MNRAS 125 141 (1963)

[56] Humphreys, R. M. AAS 19 243 (1975)

[57] Garmany, C. D. and Vacca, W. D. PASP 103 347 (1991)

[58] Denoyelles, AAS 27 3434 (1977)

[59] Haug, U. AAS 1 35 (1970)

[60] Munch, G. ApJ 125 42 (1957)

[61] Bidelman, W.P. IBVS 2514 1-2 (1984)

[62] Martin, N. AA 17 253 (1972)

[63] Nicolet, B. AAS 34 1 (1978)

[64] Conti, P.S. and Alschuler W.R. ApJ 170 325 (1971)

[65] Stone, R.P.S. ApJ 218 767 (1977)

[66] Garrison, R.F. AJ 75 1001 (1970)

[67] McCuskey, S.W., Pesch, P. and Snyder, G.A. AJ 79 597 (1974)

[68] Hiltner, W.A. and Iriarte, B. ApJ 122 185 (1955)

[69] Fernie, J.D. ApJS 52 7 (1983)

[70] Wramdemark, J. AAS 26 31 (1976)

[71] Walborn, N. R. ApJ 180 L35 (1973)

[72] from SIMBAD Database

[73] Hiltner, W.A. and Johnson, H. L. ApJ 124 367 (1956)

[74] Georgelin, Y.M., Georgelin, Y.P. and Roux, S. AA 25 337 (1973)

[75] Morgan, W.W., Code, A.D. and Whitford, A.E. ApJS 2 41 (1955)

[76] Mayer, P. and Macak, P. Bull. Astron. Inst. Czech. 22 46 (1971)

[77] Hill, P.W., Kilkenny, D. and Van Breda, I.G. MNRAS 168 451 (1974)

[78] Hill, P. W. and Lynas-Gray, A. E. MNRAS 180 691 (1977)

[79] Michigan Catalogue of Two-Dimensional Spectral Types for the HD Stars vol. 4 (1988)

[80] Johnson, H. L. et al, Com. Lun. Plan. Lab. 4 99 (1966)

[81] Guetter, H. H. PASP 80 197 (1968)

[82] Neckel, T. and Chini R. AAS 39 411 (1980)

[83] Georgelin, Y. M. et al AA 205 95 (1988)

[84] Schild, R. E. ApJ 161 855S (1970)

[85] Henderson, A. P., Jackson, P. D. and Kerr, F. J. ApJ 263 116 (1982)

VITA

The author was born in India on Nov 2, 1960. She got her B.Sc. in Physics, Chemistry and Mathematics from Osmania University, Hyderabad, India in 1980. She joined the Department of Physics and Astronomy, Louisiana State University in 1986, and got her MS degree in Physics in 1989. She worked with Dr. John Drilling toward her Doctoral degree in Astronomy.

DOCTORAL EXAMINATION AND DISSERTATION REPORT

Candidate: Jyotsna Vijapurkar

Major Field: PHYSCIS

Title of Dissertation:

A Spectroscopic Study of OB^+ Stars

Approved:

Major Professor and Chairman

George Z. Strickler

Dean of the Graduate School

EXAMINING COMMITTEE:

Arlo U. Landolt

Charles L. Perry

Date of Examination:

4/7/94